REPORT DOCUMENTATION PAGE

Form Approved OMB No. 0704-0188

1. AGENCY USE ONLY (Leave blank)	2. REPORT DATE	3. REPORT TYPE AND DATES COVERED
	13 December 2004	Fianl Report, 1 November 2003 to 1 November 2004

4. TITLE AND SUBTITLE

Modeling High Pressure Micro Hollow Cathode Discharges

5. FUNDING NUMBERS

6. AUTHOR(S)

Professor Leanne C. Pitchford

7. PERFORMING ORGANIZATION NAME(S) AND ADDRESS(ES)

CPAT
118 Route de Narbonne
Toulouse 31062
France

8. Performing Organization Report Number

9. SPONSORING/MONITORING AGENCY NAME(S) AND ADDRESS(ES

EOARD
PSC 802 Box 14
FPO 09499-0014

10. SPONSORING/MONITORING AGENCY REPORT NUMBER

SPC 03-3083

11. SUPPLEMENTARY NOTES

56 pages. Responsible person: Barrett A. Flake, telephone number +44 (0)20 7514 4285

12a. DISTRIBUTION/AVAILABILITY STATEMENT

Approved for public release; distribution is unlimited.

12b. DISTRIBUTION CODE

A

ABSTRACT (Maximum 200 words)

This report results from a contract tasking CPAT as follows: The Grantee will perform theoretical modeling of point, surface, and volume high-pressure plasmas created using Micro Hollow Cathode Discharge sources. The primary goal is to better understand the fundamental physics of these discharges in order to optimize operating conditions and develop more efficient devices.

14. SUBJECT TERMS

EOARD, Micro Hallow Cathode, Nanotechnology, Plasma dynamics, Electron beam

15. NUMBER OF PAGES

16. PRICE CODE

17. SECURITY CLASSIFICATION OF REPORT	18. SECURITY CLASSIFICATION OF THIS PAGE	19, SECURITY CLASSIFICATION OF ABSTRACT	20. LIMITATION OF ABSTRACT
UNCLASSIFIED	UNCLASSIFIED	UNCLASSIFIED	UL

Modeling High Pressure Micro Hollow Cathode Discharges

Jean-Pierre Boeuf and Leanne Pitchford
ADPA, CPAT, Université Paul Sabatier, 31061 Toulouse, France

Abstract

The objective of our work on this contract has been to use numerical modeling to develop a better understanding of the basic physical phenomena occurring in microhollow cathode discharges (MHCDs), with particular emphasis on the 2- and 3- electrode geometrical configuration used by Schoenbach et al at Old Dominion University in the USA. The same model can also be applied to other microdischarge configurations (e.g. hollow cathode tube geometries, linear slots, rf or DC excitation,…). Under high-pressure conditions the power density dissipated in the volume of these different microdischarge configurations can be very large, up to several hundreds of $kW.cm^{-3}$. MHCDs have generated considerable interest because they can operate in a *stable* regime under these high power density conditions, thus producing high-pressure non-thermal plasmas, which have many potential applications. It is very difficult to avoid instabilities that lead to a thermal plasma arc in other high-pressure DC discharge configurations. Until very recently, no theoretical or modeling results have been available, and the reasons for stability and the roles of the "hollow cathode effect", gas heating, and stepwise ionization have not been well understood. Our work provides a basis for understanding the physical mechanisms underlying this interesting discharge regime. Our model is now ready to be applied to help guide the experimental optimization of MHCDs in the context of specific applications.

This report contains an annotated compilation of manuscripts accepted for publications and conference proceedings derived from this contract over the past year. These are included here in Annexes. A full description of the numerical model and detailed preliminary results were presented in the mid-term report, also included as an Annex here. Our newest results are described in Section IV and these concern MHCDs in 3-electrode configurations. In the 3-electrode configuration, the MHCD is used as an electron source (e.g. as a cathode) and the third planar electrode (anode) is some distance away, and this configuration is of interest because of the larger volume of plasma that can be generated. Our model calculations are in excellent qualitative agreement with the experimental results of Schoenbach and colleagues in both 2- and 3-electrode systems.

Table of contents

I. INTRODUCTION

Applications or potential applications of high pressure non equilibrium plasmas are numerous: plasma processing, UV sources, chemical or bacterial decontaminations of gases, micro chemical reactors, mirror and absorbers of microwave radiations etc… Considerable work has been done in the last 10 years to design stable, high-pressure, non-thermal plasma sources.

A very promising concept for surface or volume high-pressure plasma sources is the Micro Hollow Cathode Discharge[1] (MHCD) developed by Schoenbach and coworkers at Old Dominion University. These discharges are formed through a ~ 200 μm diameter hole between two electrodes separated by a 200 μm dielectric layer. When arranged in an array, a large number of MHCDs can generate a high pressure, DC, "surface plasma" with electron densities[2] up to 10^{13} cm^{-3}. A high-pressure, DC[3], or pulsed[4], "volume plasma" can be generated with a third, planar electrode, located 1 or 2 cm from the MHCD array. In this configuration the MHCD is used as an electron source for a large volume discharge. Other high-pressure plasma sources based on this idea are described in the review paper by Kunhardt[5], and other microdischarge configurations have been discussed, for example, by Giapis and colleagues[6] and by Collins and colleagues[7].

Under the present contract we have developed a numerical model of MHCDs in the configuration of Schoenbach, and the model has been used to help develop a better understanding of the plasma generation and discharge behavior in these conditions. The model we have used to study the MHCDs is based on solutions of electron and ion transport equations coupled with Poisson's equation for the electric field including space charge and with a temperature equation for the neutral gas. In the work presented in this report, discharges in pure xenon are considered, and the excited species kinetics and stepwise ionization of metastable atoms have been taken into account in a simple and approximate way. An accurate description of the MHCD is a difficult task especially under these high power density conditions. The purpose of this work is not to provide a very accurate quantitative description of the discharge but rather to use the models to provide estimates of the main discharge and plasma parameters (charged particle densities, gas temperature, current-voltage characteristics …) and to help understand the basic mechanisms governing the MHCD devices.

We have used this model to study discharges in the following three configurations:

(a) 2-electrode MHCDs in high-pressure xenon, which have been well-studied experimentally by Schoenbach's group

(b) 3-electrode systems in high-pressure xenon where the MHCD acts as a plasma cathode for a third electrode (anode). Some experimental results in this geometry are available for argon and for air from the group of Schoenbach.

(c) low-pressure discharges in xenon in a "macrodischarge" geometry equivalent to that studied by Schoenbach and for which experiments results have recently been obtained in our laboratory.

The numerical results are in excellent qualitative agreement with experiments (except for the predicted discharge voltage vs pressure for a given current – see below). The modeling results provide an explanation for the observed structure in the voltage-current characteristic in MHCDs, which was previously attributed to the onset of the classical hollow cathode effect. The predicted steady-state characteristics of the 3-electrode configuration are also consistent with experiment. The model results provide a better understanding of this

configuration, and the model can now be used as the basis for optimizing the discharge parameters for a given application.

II. OVERVIEW OF THE MODEL

The model used is based on solutions of fluid equations in the drift-diffusion approximation for the electron and ion transport coupled with Poisson's equation. Dielectric boundary conditions are imposed on the open part of the computational domain to fix the boundary condition on the potential. This boundary is taken to be far enough from the active discharge region that it has no influence on the results. The ionization rate coefficient appearing in the electron and ion source terms is supposed to depend on the mean electron energy[8] and an equation for the electron energy is added to the system of equations to be solved.

An alternate description of the electron and ion source terms has also been developed. This is based on a Monte Carlo simulation of the high energy electrons coupled to a fluid description of the electrons and ions that contribute to the space charge. While this description is more accurate, it is much more time consuming, especially for high pressures. In our mid-term report, we concluded that the main features of the discharge development can be predicted with the simpler assumption that the source term depends on the mean electron energy. Therefore, except for the comparisons of the two different treatments of the ionization source term described in the mid-term report, all result have been obtained using the simpler model, i.e., using the mean energy parameterization of the ionization source term.

Gas heating leads to a decrease in the local neutral density and this can have important consequences on electron energy deposition in the sheath region and therefore on the sheath structure itself. We showed in the mid-term report that gas heating in a MHCD in xenon is mainly due to power deposition by ions in the sheath region (elastic and charge exchange collisions). A calculation of gas heating due to the ion current is complicated by the fact that a large part of the ion energy can be released on the cathode (by ions or fast neutrals) instead of in the gas[9]. A detailed description of the gas heating by the ion current would require a Monte Carlo simulation of the ions and of the fast neutrals created in ion/neutral collisions in the sheath. Rather than include this level of detail in the present model, we consider that a given, fixed fraction of the ion heating is converted locally into gas heating, the rest being deposited on the cathode which is fixed at 300K. Using this as a source term, the gas temperature is obtained from the heat equation. We show below that this approximation for the gas heating source term is not a factor limiting the quantitative accuracy of the model. Electron heating of the gas is taken into account but is negligible for our conditions. Note that in molecular gases gas heating can also be caused by R-T and V-T (rotational or vibrational to translational) energy transfer, and thus gas heating due to the electron current is likely to be much more important. Gas flow is not taken into account, and if we continue with modeling MHCDs, incorporating gas flow will be a next objective.

To estimate the contribution of the xenon excited species to the overall ionization balance and the contribution of molecular ion formation and recombination to the overall electron loss, a very simple model kinetic is used. The species considered in the simulation are electrons, atomic ions, molecular ions, and metastable atoms. The model of the xenon metastable density is based on ref. 10, but simplified by assuming that the ratio of resonance to metastable atoms is constant.

The numerical implementation of this physical model was described in detail in the annex of our mid-term report, which is attached as Annex I. This model was adapted recently to allow for non-uniform computational grids, which improves the accuracy and efficiency of

the calculations. Calculations shown below were performed on a 100x100 nonuniform grid for the 2-electrode geometry and with a 200x100 nonuniform grid for the 3-electrode geometry. The computational time typically required for each point in the results shown below is several hours (2-electrode geometry) to some 10's of hours (3-electrode geometry) on a high-performance PC.

III. BASIC PROPERTIES OF THE 2-ELECTRODE MHCD

The mid-term report presents results showing plasma parameters (electron and ion densities, metastable densities, ionization source term, gas temperature) over a range of conditions. We have made some changes in the numerical implementation of the model that leads to small changes in the values of these parameters, but the results in the mid-term report are still representative of their predicted values and the trends reported in the mid-term report remain valid.

In the rest of this section we summarize results obtained in the past six months.

a) Interpretation of structure in the V-I characteristic

An article, co-authored with K.H. Schoenbach and describing our main results in MHCDs in 2-electrode systems and in pure xenon, has been accepted for publication in Applied Physics Letters. This manuscript is attached here as Annex II.

The main point of this article is to present a new theoretical interpretation of the voltage maximum observed in the experimental voltage-current (V-I) characteristics of Schoenbach et al and others. Our conclusion is that this structure is due to a transition between an abnormal glow discharge localized inside the hollow cathode structure to a normal glow discharge spreading out along the back surface of the cathode. That is, with increasing current in MHCDs there is a transition from abnormal discharge inside the hollow cathode to a normal glow discharge where much of the current is drawn through the outer surface of the cathode. This transition manifests itself in the shape of the voltage-current characteristic – voltage increases at low current and then reaches a peak and saturates or decreases somewhat at higher current. This structure has been previously attributed to the onset of the classical hollow cathode effect (enhanced ionization due to pendulum electrons oscillating between opposite sheaths in the hollow cathode). We have shown that the classical hollow cathode effect does *not* occur for the experimental conditions of Schoenbach and for gas pressures greater than 100 torr even when the rarefaction due to gas heating is taken into account.

Although the model used here is approximate and more work needs to be done to improve the quantitative predictions, this conclusion is significant for its implications in mechanisms of stability in MHCDs. At high current, the power density inside the hollow cathode does not increase significantly with increasing current, provided that the discharge can continue to spread on the outer surface of the cathode. Consequently, the gas temperature and electric field at the cathode surface both tend to saturate with increasing current as long as there is available cathode surface for the discharge to spread. This is important because increases in either of these quantities can trigger instabilities.

b) Sensitivity to input parameters

The baseline conditions used for the results in Section IIIa were : pure xenon at 100 torr; secondary electron emission coefficient due ion bombardment, 0.002 and due to metastable bombardment, 0.005; fraction of ion power deposited locally in gas heating, 25%, surface temperatures, 300K; and ratio of resonance to metastable density, 0.1. The geometry we used

is as follows : cathode hole diameter is 240 microns, the width of the dielectric is 250 microns, and the thickness of each of the electrodes is 100 microns.

Some parametric calculations were presented in the mid-term report. We made further calculations to test the extent to which estimated values of the input parameters affect the calculated voltage-current characteristics.

secondary electron emission coefficient

Critical parameters are the coefficients defining the electron emission from the cathode surface due to ion bombardment (γ_{ion}) and to metastable bombardment (γ_{meta}). These quantities are not well known and the values we have used for the baseline conditions were estimated by fitting to the experimental results of Schoenbach et al. Fig. III.1 shows V-I characteristics calculated for different assumed values of the secondary electron emission coefficients, γ. The shape of the characteristic is not too dependent on the exact value of this parameter, but the magnitude of the voltage is quite dependent on γ. At the voltage peak and for the baseline conditions, the plasma density is approximately $3\ 10^{13}$ cm^{-3}. There is not a large increase in this peak density with increasing current past the peak because an increase in current is achieved by an increase in the electron emitting of the cathode surface and not by an increase in the current density. Neither is there a large change in the plasma density at the voltage peak with changes in the secondary electron emission coefficients over the range shown below.

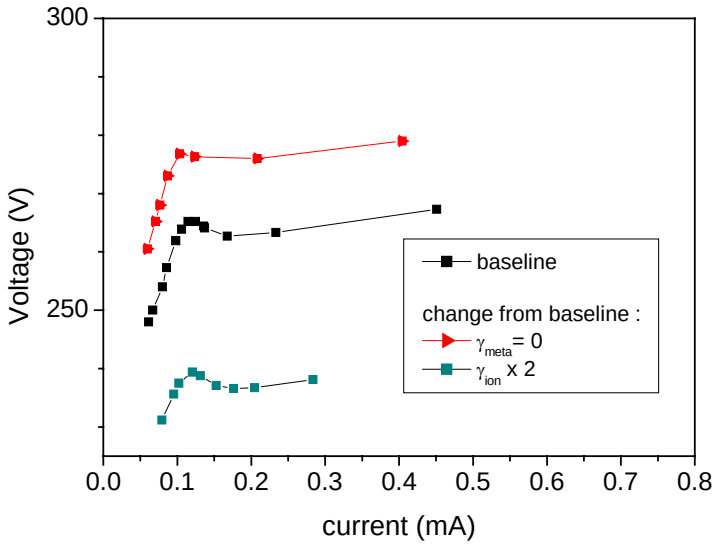

Fig. III.1. Voltage-current characteristics in MHCDs in xenon for different assumptions on secondary electron emission. Same geometry as in section II (figure 1 of Annex I), and for the baseline conditions at 100 torr.

fractional ion energy deposited in gas heating

We have supposed for most of our calculations that the fraction of the power absorbed by the ions that converted locally to gas heating through ion/neutral collisions, F, is 25%. We know from our previous calculations for other glow discharge conditions[9] that the ions, and especially fast neutrals created in the ion/neutral collisions, carry a significant fraction of their energy to the cathode. The value of 25% that we use here is an estimate based on previous calculations in glow discharge in argon and neon. A Monte Carlo simulation of the ions and

the fast neutrals generated by the ion current in the sheath would be necessary to improve this estimate. The voltage-current characteristics calculated assuming that either 0 or 100% of the ion power is converted locally to gas heating are shown in fig. III.3 and compared to the baseline conditions at 100 torr. The overall discharge behavior and the shapes of the V-I curves do not depend on F, but the magnitude of the voltage for a given current does. The current at which the voltage peaks also changes with F because of increasing gas temperature (lower gas density) for higher F. The peak gas temperatures are 303 K, 450 K and 750 K for F = 0, 25 and 100%, respectively. The value of F does not affect very much the peak electron density for a given current, but it does influence the spatial distribution of the plasma density. At this stage of model development, our opinion is that improving the description of the gas heating due to ion/neutral collisions is not a priority issue.

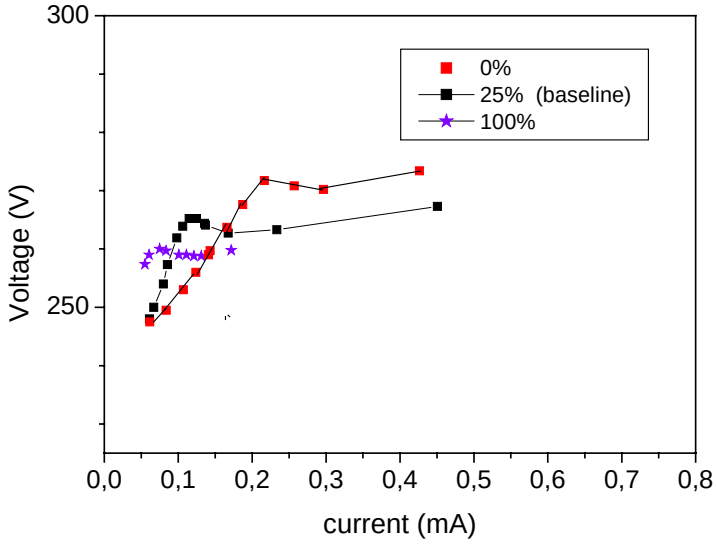

Fig.III.2. Voltage-current characteristics calculated for different assumptions for the fraction of the ion power absorbtion converted locally to gas heating. The conditions are otherwise the same as for the baseline case in fig. III.1.

gas pressure

Consistent with the conclusion in our mid-term report, the only significant difference between the trends predicted in the model calculations and those observed experimentally is in the pressure dependence. For a given current, the voltage is lower at a higher pressure in the experiments, whereas it is the opposite in the model results. We do not yet understand the reasons for this difference (which is seen again at low pressure – see section V below). Our premise is that photoemission, not included in the model, could lead to the observed pressure dependence. More work is needed to understand the reasons for the predicted pressure dependence and to improve the model on this point.

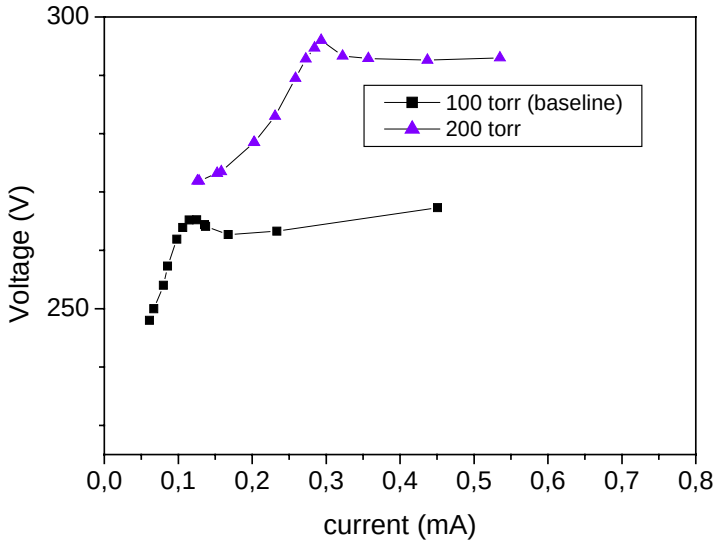

Fig. III.3. Voltage-current characteristic calculated for pure xenon at 100 and 200 torr, same conditions as fig. III.1 (baseline conditions).

IV. 3-ELECTRODE MHCD CONFIGURATION

Schoenbach et al have demonstrated that a high-pressure, DC[3], or pulsed[4], "volume plasma" can be generated with a third, planar electrode, located 1 or 2 cm from the MHCD array. In this configuration the MHCD is used as an electron source for a large volume discharge. We have obtained some preliminary results in this configuration, which help understand the reasons for the observed behavior.

The three electrodes are shown in figure IV.1, which is taken from Stark and Schoenbach (ref. 3). The electrodes are designated C, cathode; A1, the middle electrode (the anode in the MHCD); and A2, the third electrode. From experiment, it is known that the electron current flows either to A1 or to A2, depending on the total discharge current and the value of the voltage applied to A2. At low discharge current, the third electrode A2 is not seen by the discharge and all the electron current is collected by A1. The current at which the transition from A1 to A2 occurs depends on the voltage applied to A2. Not surprisingly, a higher voltage on A2 causes a transition at a lower current.

The baseline conditions of Section III were used for all calculations presented in this section: pure xenon at 100 torr; secondary electron emission coefficient due ion bombardment, 0.002 and due to metastable bombardment, 0.005; fraction of ion power deposited locally in gas heating, 25%, surface temperatures, 300K; and ratio of resonance to metastable density, 0.1. The dimensions are listed in Table I; the MHCD dimensions are the same as for the baseline conditions. For numerical consistency, the same computational grid was used in the MHCD region and another 100 axial grid points were added for the discretization of the A1-A2 volume (i.e. a 200x100 nonuniform grid was used in these calculations).

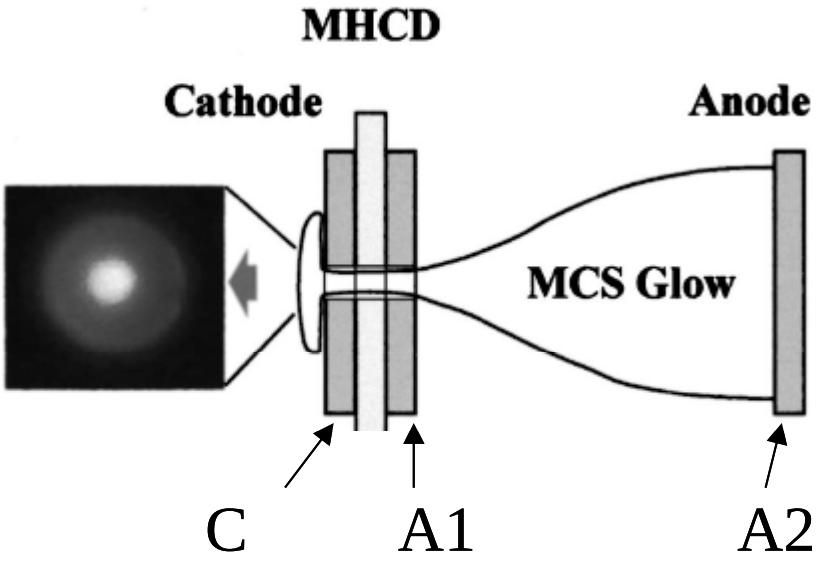

Fig. IV.1. Schematic of 3-electrode geometry from Stark and Schoenbach (ref. 3). The MHCD is used as an electron source for the Microhollow Cathode Sustained (MCS) glow.

	Dimensions (microns)
Cathode hole diameter	280
Thickness of electrodes C and A1	100
Thickness of MHCD dielectric	250
Separation A1-A2	1000

Table I. Dimensions used for calculations in 3-electrode configurations

The distance separating A1 and A2 is only 0.1 cm for the calculations reported here, compared to some 0.8 cm in the experiments of Schoenbach. A few calculations were performed for a 0.3 cm distance, but these are very time consuming and results from these are not qualitatively different from results with a smaller spacing. Therefore, all results reported here are for 0.1 cm spacing where we have a more complete set of results.

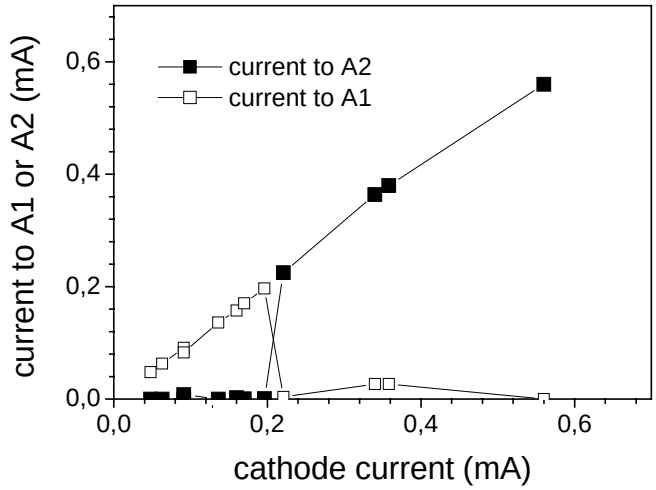

Fig. IV.2 Current collected by electrodes A1 and A2 as a function of total discharge current in the 3-electrode geometry. The voltage on A2 is between 300 and 306V.

The results of our calculations in the 3-electrode configurations are summarized in fig. IV.2. Here we show the currents collected by electrodes A1 and A2 as a function of total discharge current (the current to the cathode C) and for a voltage on V2 of about 305 V (from 300 to 306 V). The current is adjusted either by changing the series resistance or by changing the voltage on A1; the calculated voltage on A1 for a given discharge current is shown in fig. IV.3. Consistent with experiment, we find that all the electron current is collected by the anode A1 for low total current and by A2 for high current. That is, at low current, the third electrode has no effect on the discharge behavior. With increasing current there is an abrupt transition to a discharge between a MHCD discharge and a discharge between electrodes C and A2. The transition occurs very abruptly and at about 0.2 mA for the conditions studied here.

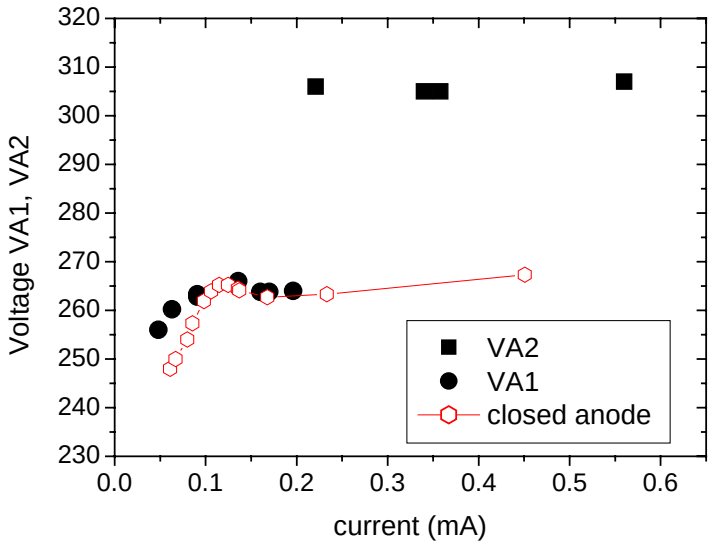

Fig. IV.3. Calculated current-voltage characteristic for 3-electrode geometry. The symbols in red correspond to the calculated characteristic for a 2-electrode geometry with a closed anode, as reported in Annex II.

The voltage-current characteristic for the 3-electrode geometry is shown in fig. IV.3. The low current portion (discharge between C and A1) is essentially the same as for a 2-electrode system calculated with a closed anode (red symbols). We have not attempted to understand the reasons for the small differences in the operating voltage at low current between open and closed anode geometries. The voltage on VA1 for points after the transition (0.2 mA) was not a well controlled parameter in our calculations – in retrospect, we should have chosen to keep constant the difference between the VA1 and VA2 (although this is difficult to adjust). However, based on results in this geometry and on an incomplete set of results for other electrode dimensions (not shown here), it seems that the voltage on A1 is not very important once the transition to a discharge occurring between C-A2 occurs.

We will now look in more detail at the plasma parameters for three points (0.09, 0.2 and 0.22 mA) along the characteristic shown in fig. IV.3. These are representative of three different regions: (a) 0.09 mA: abnormal glow between electrodes C and A1, (b) 0.2 mA: normal glow along the outer face of the cathode C and A1, and (C) 0.022 mA: a normal glow discharge between C and A2. The first two regions are the same are we have described above for the 2-electrode systems.

The electron, ion and metastable densities are shown in figs. IV.4 (a) and (b) for the two points at 0.09 and 0.2 mA. For the 0.09 mA point, the discharge is in the abnormal glow regime (increasing current and voltage), as described in Annex I and II. The discharge is localized inside the cathode hole and is the same as in the 2-electrode geometry with a closed anode. With increasing current, the discharge starts to spread along the outer face of the cathode and, associated with the onset of electron emission from the outer face of the cathode is a decrease in the operating voltage of the discharge. The decrease is only a few volts for the conditions here. Again, this is the same result that we found for the 2-electrode, closed anode configuration. For both points, there is very little ionization in the volume between A1 and A2. The metastable density peaks off-axis and inside the cathode hole at 0.09 mA, and the peak at 0.2 mA has moved to the volume outside the MHCD. It is interesting to note that

the metastable density in the volume A1-A2 is larger for the lower current point. This is because the region where metastables are produced is nearer the A1-A2 volume for the 0.09 mA point, whereas it is mainly in the volume outside the cathode face for the 0.2 mA point. Electron quenching is a major loss process for the metastables where the electron density is large (inside the cathode hole and along the outer face). This quenching process is practically zero in the A1-A2 volume because there are so few electrons, and the only loss processes in this region are excimer formation or quenching at the walls. The atomic ions are localized close to the cathode surface, near where they are created (see below). Molecular ions, created in 3-body collisions of atomic ions and the neutral atoms, are more broadly distributed in space.

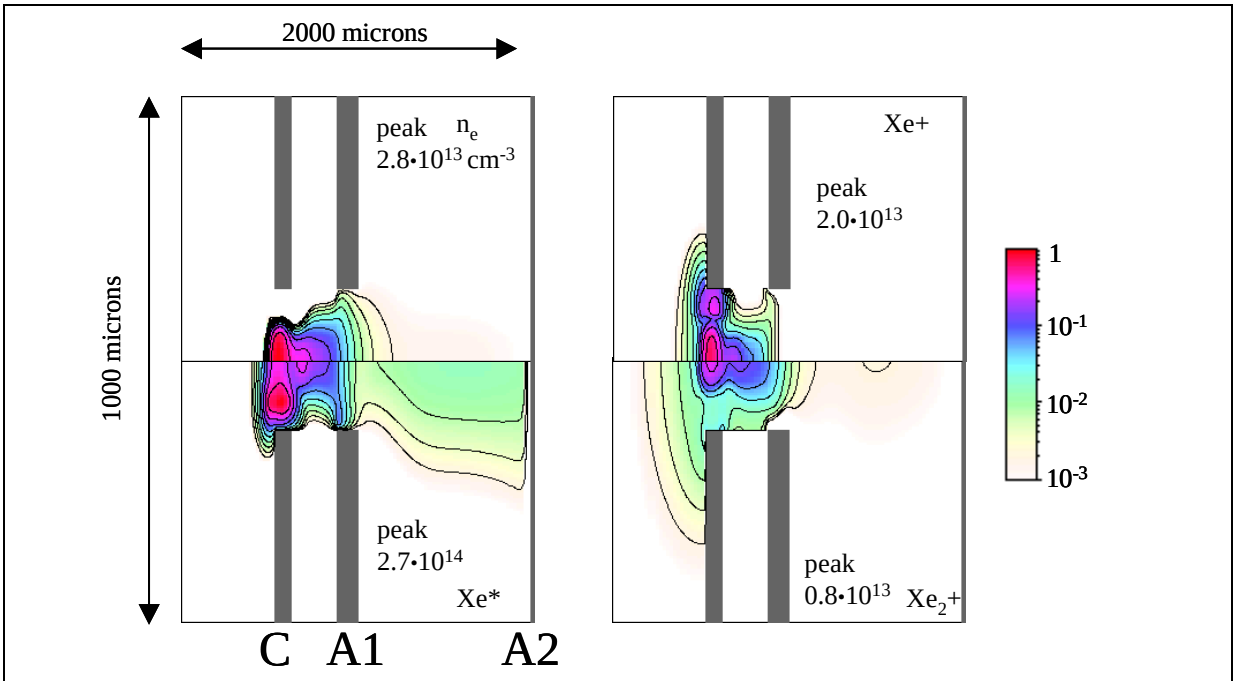

a) 0.09 mA

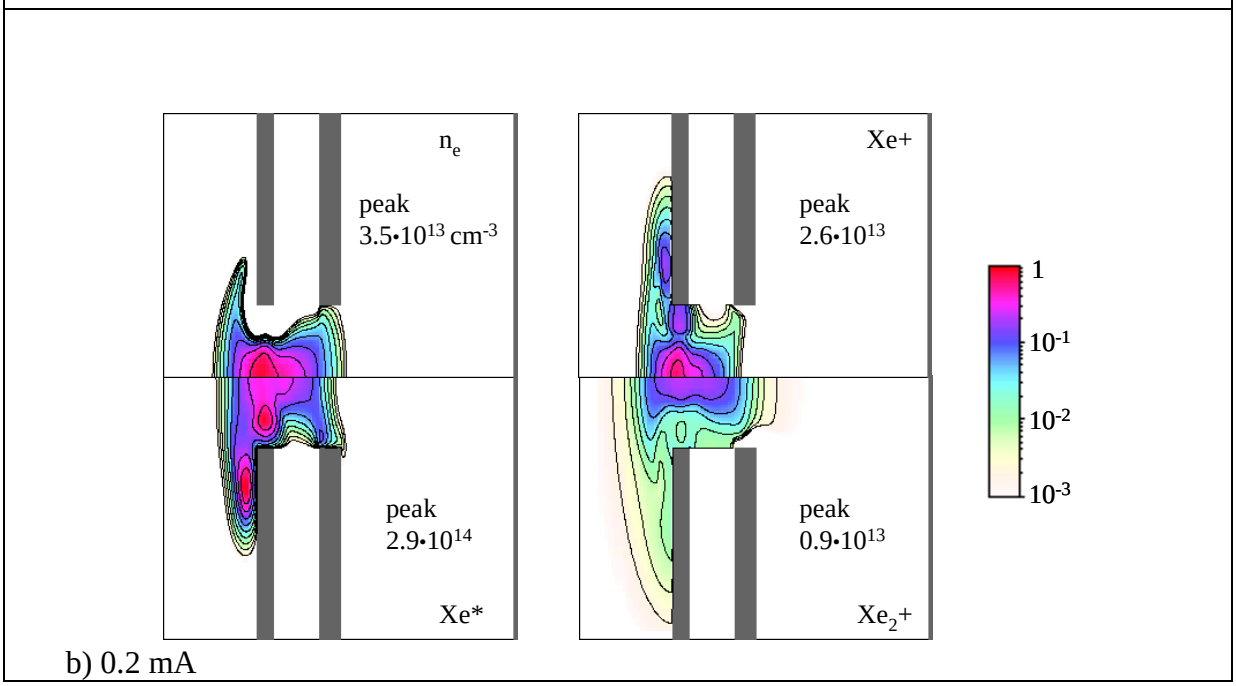

b) 0.2 mA

Fig. IV.4 Calculated electron, ion and metastable densities (a) for the point at 0.09 mA and (b) for the point 0.2 mA in fig. IV.2. The charged particle densities at each current are plotted on the same scale (relative to the peak electron density) and the density peak is indicated on each panel. The contours are equally spaced on the log scale shown in the color bar on the right.

The direct and stepwise ionization rates and the spatial distribution of the potential are shown in fig. IV.5, also for the 0.2 mA point. Direct ionization is much more important than the stepwise ionization, but direct ionization occurs only in the sheath surrounding the cathode, whereas stepwise ionization is more extended in space, consistent with the fairly broad spatial distribution of the metastables.

The distribution of the potential is also shown in fig. IV.5 for 0.2 mA. The values of the electrode potentials are 0, 264 and 300 V, respectively for electrodes C, A1 and A2. Calculations using different values of the potential of A2 (up to 340 V) yield the same total discharge current. We see that the contours of constant potential are such as to push the electrons toward the surface of anode A1.

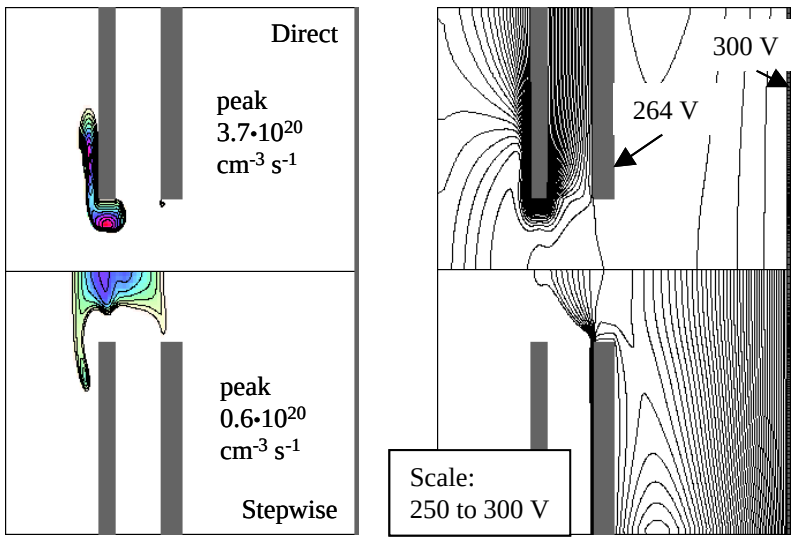

Fig. IV.5. Direct and stepwise ionization source terms and spatial distribution of the potential. The source terms are plotted on the same scale (relative to the peak direct ionization), and the ten contours are equally spaced on a log scale. The color bar is shown in fig. IV.4. Thirty equally space contours between 0 and 300 V are shown for the potential in the upper panel on the right. Fifty equally spaced equipotential contours are plotted between 250 and 300 V in the lower right panel.

We will now compare the results at 0.2 mA with those for a slightly higher current, 0.225 mA. At this point the discharge occurs between the cathode C and the anode A2. The electron, ion and metastable densities for this point are shown in fig. IV.6. The peak values of these densities are not very different from the case at lower current, but their spatial distributions are quite different. It is obvious from these distributions that the discharge is occurring between C and A2 – for a slight increase in the discharge current, the metastable

and charged particle densities are significant in the volume between A1 and A2 in contrast to those shown in fig. IV.4 where this volume was void of excitation/ionization.

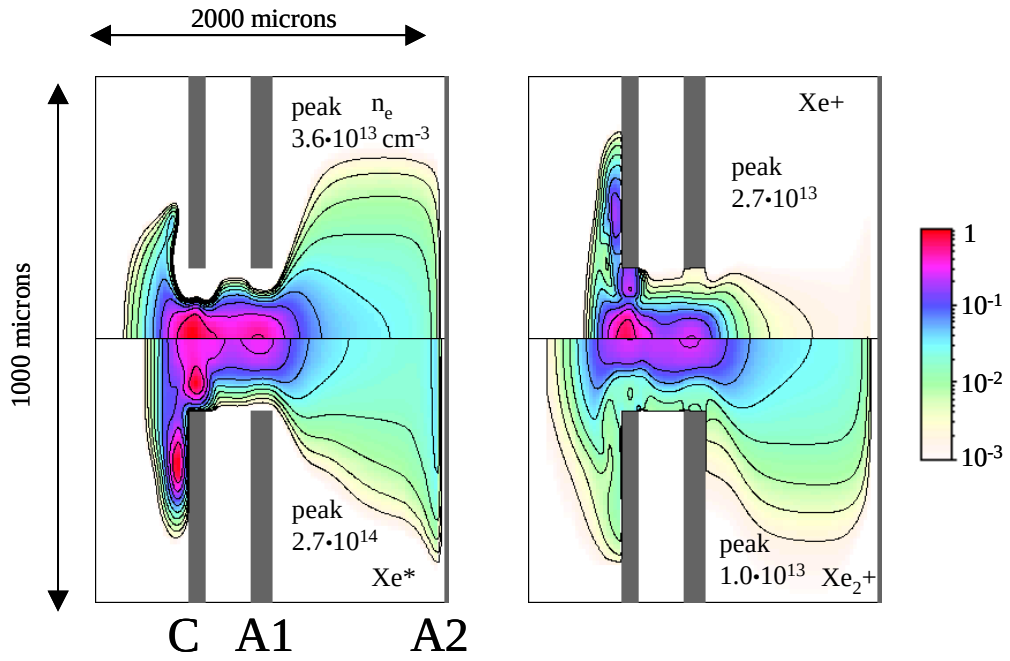

Fig. IV.6. Calculated electron, ion and metastables densities for the point at 0.225 mA in Geometry 2. The scale for the charged particle densities is the same (normalized to the peak electron density) and the contours are equally spaced on a log scale. The color scale is shown in the bar on the right.

The direct and stepwise ionization source terms for the point at 0.225 mA are shown in fig. IV.7. These are not very different from the source terms at 0.2 mA, although they are somewhat more extended along the back surface of the cathode.

The equipotential contours for the 0.225 mA point are also shown in fig. IV.7. For these calculations, the potential of anode A2 is 306 V, and the potential of A1 is 223 V (fixed by the external circuit). Between the point at 0.225 mA and 0.56 mA, the highest current point in fig. IV.2, the potential of anode A2 is constant at about 305 V, while the potential of anode A1 decreases to 77 V. As mentioned above, in retrospect, we should have controlled differently the value of the potential on electrode A1, but our results do not suggest that this is significant. The potential distribution for the 0.225 mA point in the region of the cathode hole is such as to focus electrons towards the axis and towards A2.

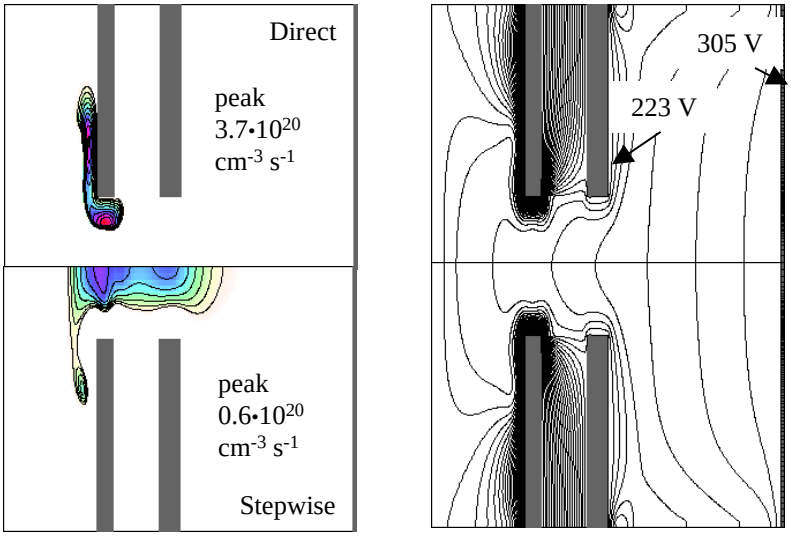

Fig. IV.7. Direct and stepwise ionization source terms and spatial distribution of the potential for the point at 0.225 mA. The source terms are plotted on the same scale (relative to the peak direct ionization), and the ten contours are equally spaced on a log scale. The color bar is shown in fig. IV.4. Thirty equally space contours between 0 and 305 V are shown for the potential.

The gas temperatures profiles were presented in the mid-term report for calculations in the 2-electrode geometry. For the cases reported here, we find essentially the same profiles (peaks near the peak of the direct ionization source terms) with peak gas temperatures of about 450 K. The transition to a discharge between electrodes C and A2 causes no significant changes in these gas temperature profiles.

The conclusions from these calculations are as follows - The calculations are consistent with experiment in the prediction that the discharge jumps from anode A1 to anode A2 with increasing current. This jump is abrupt. We can consider that the transition occurs when the conditions from breakdown in region A1-A2 are reached. Breakdown occurs between the plasma created inside the MHCD and the anode A2. Thus, the prerequisite for the discharge C-A2 is first a discharge inside the MHCD between C and A1. The conditions for breakdown between the MHCD and A2 depend on the MHCD current (the extension of the plasma region into the A1-A2 gap), the potential on A2, the gas pressure and the distance between A1 and A2. When breakdown occurs between the plasma and A2, the anode A1 no longer plays a role.

Thus, it appears that the initiation of a discharge between C and A2, proceeding in two stages and starting with the MHCD between C and A1, is a means for avoiding streamer breakdown and inevitable transition to a thermal plasma arc.

V EQUIVALENT GEOMETRY – LOW PRESSURE

Experiments in our laboratory in a discharge configuration equivalent to the MCHDs of Schoenbach were performed. By "equivalent" we mean that the pd product (pressure x dimensions) is the same as in the MCHDs, but the gas pressure is 50 times lower. Thus, the dimensions are on the order of 1 cm and the gas pressure is several torr. V-I characteristics were measured for several different pressures and the emission intensity was photographed (facing the flat surface of the cathode) for different conditions. These results were compared

with calculations. Gas temperature and degree of excitation are significantly lower at than in the high-pressure cases presented above.

These results have been submitted to special issues on Images in Plasma Physics that will be published in the IEEE Transactions on Plasma Science in 2005. The manuscript is attached here in Annex III. This work was also presented at the Gas Discharge meeting in Toulouse in September 2004, and the article from that conference is attached here in Annex IV.

The main conclusions from this work can be summarized as follows. The overall discharge behavior is the same at low pressure and at high pressure, as expected from pd (gas pressure x discharge dimensions) scaling. The numerical model provides a good description of the discharge behavior for both high pressure and low-pressure configurations. Better values of the input parameters, and in particular the secondary electron emissions coefficients are needed for improved quantitative predictions. The gas temperatures in these low-pressure discharges are predicted to increase from 300 K to at most 320 K. This is in sharp contrast to the results at 100 torr where the peak gas temperatures are predicted to be about 450 K or 700 K (assuming 25% or 100%, respectively, of the power deposited in the ions goes into gas heating). The contribution of stepwise ionization to the total ionization rate is insignificant in the low-pressure discharges, whereas it is some 10 to 20% of the total ionization for the MHCDs at 100 torr. Consistent with the results of Schoenbach in MHCDs, we find that for a given current, the measured discharge voltage is lower at higher pressure (in the range of 1 to 6 torr). As we found for MHCDs in high-pressure xenon, our model results predict the opposite trend and we do not yet understand the reason for this discrepancy.

VI CONCLUSIONS AND FUTURE PLANS

Over the course of this contract, we have developed a numerical model of MHCDs, which describes the basic physical mechanisms in this novel discharge configuration. The experimentally observed voltage maximum was previously attributed to the onset of the classical hollow cathode effect (enhanced ionization due to electrons oscillating between opposite cathode sheaths). Our model provides an different explanation - that the structure observed experimentally in the V-I characteristics in MHCDs reflects a transition from an abnormal glow discharge (positive slope) at low current to a normal glow discharge (zero or very small slope) at high current. This geometrical effect is the main reason for stability of high-pressure discharges in microhollow cathode geometries. Instabilities are triggered by increasing gas temperature and/or by high electric fields at the cathode surface. Both of these quantities tend to saturate with increasing current in MHCDs, whereas these quantities usually increase until an instability is provoked in a planar discharge geometry, for example. We are led to the conclusion that stable nonthermal discharges can be more easily maintained at high pressure is the cathode geometry is such that the discharge can spread along the surface after breakdown occurs. The geometries studied by Schoenbach and his colleagues as well as the configurations studied by the groups of Collins[7], Giapis[6], and Simonchik[11] and others fulfill this requirement and are unusually stable. The 3-electrode geometry is another interesting configuration for generating and maintaining high-pressure nonthermal plasmas.

There are a number of possible directions for further modeling work in MHCDs. Some application areas we would like to pursue are the following:

- Discharges in high pressure xenon or in rare gas mixtures containing xenon are of interest in the context of UV and VUV generation. Numerical experiments on MHCDs in stacks or in 3-electrode systems could help identify an optimum configuration for efficient UV generation. A model of radiation transport including photoemission from the cathode

surfaces is needed to go further in this direction. We will be pursuing this application area in collaboration with Prof Klaus Frank at the University of Erhlangen, Germany, who has received a grant for travel funds for a student exchange with our laboratory.

- The generation of stable, non-thermal plasmas in air has been the subject of previous Air Force projects, and using MHCDs in this context is still of interest. We have limited our work so far to discharges in xenon where the plasma chemistry is relatively simple, although still approximate. Our model is suitable for studying MHCDs in air, but before doing so, it will be necessary to develop a simple model of the ionization balance specific to the gas mixture. There is a huge amount of literature on air plasma chemistry, for example, and the problem is to extract from this a simple model of the ionization balance in a nonthermal plasma, which could then be used as input to our MHCD model. A further complication that would have to be considered in extending our calculations to air or to molecular gases in general is gas heating by the electron current. Gas heating is much more complicated in molecular gases because of the efficient V-T and R-T (vibrational to translational and rotational to translational) energy transfer process. That is, gas heating by the electron current, negligible in xenon, can become significant for molecular gases, and including this effect in our model would also require a much more detailed treatment of the plasma chemistry.

- An interesting category of applications involves using MHCDs as micro-chemical reactors. The plasma conditions (high pressure, high power, proximity of the walls) that can be achieved in MHCDs are difficult or impossible to obtain with other plasma sources, and this offers unique possibilities for generation of high fluxes of radicals. In addition to the plasma chemistry, gas flow becomes an important consideration for this category of applications. Gas flow influences the plasma through its effect on the plasma composition and especially on the gas temperature; the estimated flow rates are too small to influence the charged particle transport. We have recently developed in our group a module that can be coupled to the MHCD model fairly easily.

- Related to the above is the possibility of generating a high yield of $O_2(^1\Delta)$ in a MHCDs. This is interesting in the context of electric discharge pumping of COIL lasers. We submitted a white paper on this topic to AFOSR, EOARD and AFRL (Albuquerque) in September.

- Other discharge configurations can be studied with our model or slight extensions of our model. Collins and colleagues have shown that discharge stability can be improved even further by using rf excitation (13.56 MHz). In contrast to the work of Schoenbach, Collins uses a linear geometry and a uniform, stable discharge is obtained along the length of a 30 cm (or more) cathode. Giapis et al have demonstrated stable discharge operation at atmospheric pressure using long tubular cathodes (metallic capillaries) facing a planar anode, and especially long life is observed in this configuration. Other stable discharge configurations based on micro-geometries are perforated dielectric coverings on planar cathodes or dielectric capillaries extending from the planar cathode surface.

REFERENCES

[1] KH Schoenbach, A. El-Habachi, W. Shi, and M. Ciocca, *High pressure hollow cathode discharges*, Plasma Sources Sci. Technol. **6**, 468 (1997)

[2] KH Schoenbach, A. El-Habachi, MM Moselhy, W Shi, and RH Stark, *Microhollow cathode discharge excimer lamps*, Phys. Plasmas **7**, 286 (2000).

[3] RH Stark and KH Schoenbach, *Direct high pressure glow discharges*, J. Appl. Phys. **85**, 2075 (1999)

[4] RH Stark and KH Schoenbach, *Electron heating in atmospheric glow discharges*, J. Appl. Phys. **89**, 3568 (2001)

[5] EE Kunhardt, *Generation of large volume, atmospheric-pressure, non-equilibrium plasmas*, IEEE Trans Plasma Sci. **28**, 189 (2000)

[6] R.M. Sankaran and K. P. Giapis, *Hollow cathode sustained plasma microject: characterization and application to diamond deposition*, J. Appl. Phys, **92**, 2405 (2004).

[7] Z. Yu, K. Hoshimiya, J. D. Williams, S. F. Polvinen and G.J. Collins, *Radio-frequency-driven near atmospheric pressure microplasma in a hollow slot electrode configuration*, Appl. Phys. Letts **83**, 852 (2003).

[8] J. P. Boeuf et L. C. Pitchford, *Two-dimensional model of a capacitively coupled rf discharges and comparisons with experiments in the Gaseous Electronics Conference reference reactor*, Phys Rev E **51,** 1376 (1995).

[9] I. Revel, L. Pitchford, J.P. Boeuf, *Calculated gas temperature profiles in argon glow discharges*, J. Appl. Phys. **88**, 2234 (2000)

[10] L.C. Pitchford, J. Kang, C. Punset, and J.P. Boeuf, *Calculated characteristics of rf plasma display panel cells including the influence of xenon metastables*, J. Appl. Phys. **92**, 6990 (2002)

[11] V.I. Arkhipenko, A.A. Kirillov, L.V. Simonchik, S.M. Zgirovskii, Cathode fall parameters of a self-sustained normal glow discharge in atmospheric-pressure helium, Plasma Phys. Report **28**, 858 (2002).

ANNEX I : Mid-term grant report

Grant 033083

Mid-term report 31 March 2004

ABSTRACT

A model has been developed and used to clarify the physical mechanisms occurring in Micro Hollow Cathode Discharges (MHCD) operating at high pressures. Under high pressure conditions the power density dissipated in the volume of the micro-discharge can be very large, up to several hundreds of $kW.cm^{-3}$. The micro-discharges can operate in a stable regime under these high power density conditions, and therefore have many potential applications. The reasons for stability, the role of the "hollow cathode effect", and the excited species chemistry are not clearly understood. The model is used to clarify the influence of temperature effects, stepwise ionization, and pendulum electrons oscillating in the hollow cathode, on the discharge properties and characteristics. Preliminary results are presented for discharges in pure xenon (which have been well studied experimentally by the Schoenbach's group).

I. INTRODUCTION

Applications or potential applications of high pressure non equilibrium plasmas are numerous: plasma processing, UV sources, chemical or bacterial decontaminations of gases, micro chemical reactors, mirror and absorbers of microwave radiations etc… Considerable work has been done in the last 10 years to design stable, high-pressure, non-thermal plasma sources.

A very promising concept for surface or volume high-pressure plasma sources is the Micro Hollow Cathode Discharge[1] (MHCD) developed by Schoenbach and coworkers at Old Dominion University. These discharges are formed through a ~ 200 μm diameter hole between two electrodes separated by a 200 μm dielectric layer. When arranged in an array, a large number of MHCDs can generate a high pressure, DC, "surface plasma" with electron densities[2] up to 10^{13} cm^{-3}. A high-pressure, DC[3], or pulsed[4], "volume plasma" can be generated with a third, planar electrode, located 1 or 2 cm from the MHCD array. In this configuration the MHCD is used as an electron source for a large volume discharge (other high pressure plasma sources based on this idea are described in the review paper by Kunhardt[5]).

The experimental work of Schoenbach and coworkers has provided very useful insight in the discharge regime and plasma characteristics. However we believe that there is a lack of basic understanding of the physics of these systems. A deeper understanding of the discharge and plasma properties would certainly help finding optimum operating conditions or improvements of the concepts.

The model we have used to study the MHCDs is based on solutions of electron and ion transport equations coupled with Poisson's equation and with a temperature equation for the neutral gas. Bulk electrons and ions are simply described by a fluid, drift-diffusion model, but fast electrons emitted at the cathode surface under ion bombardment and accelerated in the sheaths are described with a Monte Carlo simulation (hybrid model of electron transport). We

also developed and used a simpler and faster model based on a fully fluid description of electron transport (fluid energy equation is solved for the electrons and the ionization rate is supposed to depend on the mean electron energy). Although this model cannot describe the hollow cathode effect, it may give reasonable trends when this effect is not dominant. In the work presented in this report discharges in pure xenon are considered, and the excited species kinetics and stepwise ionization of metastable atoms have been taken into account in a simple and approximate way. An accurate description of the MHCD is a difficult task especially under these high power density conditions. The purpose of this work is not to provide a very accurate quantitative description of the discharge but rather to use the models to provide estimates of the main discharge and plasma parameters (charged particle densities, gas temperature, current-voltage characteristics …) and to help understand the basic mechanisms governing the MHCD devices.

The details of the model are given in Appendix A1.

Some preliminary results are shown in section II.

II. PRELIMINARY RESULTS

The preliminary results shown here are related to pure xenon. The geometry of the device is shown in Fig. 1 and is similar to the geometry used in the experimental work of Schoenbach et al.. The gas pressure was varied from 15 torr up to 200 torr.

The questions we want to address are the following:

1) Is the hollow cathode effect important in the conditions of Schoenbach et al. and does it play an important role in the properties of the MHCDs ?
2) How high is the gas temperature and what are the mechanisms which control it (i.e. which prevent the glow to arc transition) ?
3) What is the role of the excited species kinetics in the particular case of xenon (or in other rare gases) ?

In order to better understand the role of temperature, stepwise ionization and hollow cathode effect, we compared simulation results assuming fixed or calculated gas temperature, with or without including stepwise ionization, with the fully fluid model or with the hybrid model (the fluid model cannot describe the hollow cathode effect).

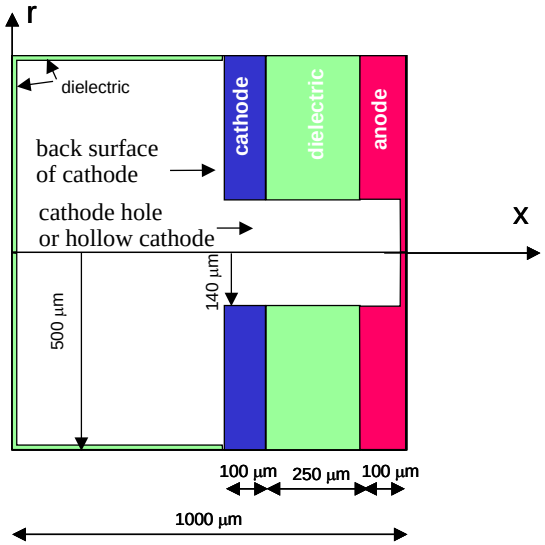

Figure 1: Geometry of the simulated MHCD. Most of the simulations were performed in a 100x100 uniform grid.

II.1 Hollow cathode effect

The hollow cathode effect is generally attributed to the trapping and oscillations of fast electrons between the sheaths formed along the surface of a hollow cathode. These oscillations increase the residence time of fast electrons in the sheaths and therefore increase the number of ionization events in the sheath region. Electrons generated by ionization within the sheath can themselves be accelerated by the sheath electric field and perform ionization collisions. It is therefore clear that the "pendulum oscillations" of the fast electron between the sheaths lead to a global enhancement of the ionization efficiency for a given sheath voltage (i.e. an increase of the current density at constant voltage). The trapping and reflections of photons in the hollow cathode geometry is also often mentioned as a possible cause of the hollow cathode effect. Some simple conditions must be fulfilled to obtain a substantial hollow cathode effect due to electron oscillations between the sheaths: 1) the energy relaxation length of the fast electrons should be of the same order as the distance between cathode surfaces, and 2), the sheath length must not be too small with respect to the distance between the facing sheaths.

In the geometry of Fig. 1 and for a pressure of 100 torr, the product of the pressure p by the diameter D of the hole is 2.8 torr.cm and the energy relaxation length (typically several electron mean free paths) is on the order or less than 1 torr.cm at 300 K (it actually depends on the electron energy and thus on the sheath voltage). One can therefore conclude that the hollow cathode effect is probably not very important at 100 torr and certainly negligible above 300 or 400 torr. The correct scaling factor is actually the gas density and not the gas pressure, and the above estimations, which assume a gas temperature of 300 K, may be wrong if the gas temperature is much larger than 300 K. More quantitative arguments are given below.

Figures 2 and 3 show the results of the hybrid model (in pure xenon, assuming only direct electron impact from the ground state) in the geometry of Fig. 1 and for a gas pressure of 30 torr and for 3 points on the V-I characteristics. Stepwise ionization is not included in these calculations but the gas temperature is self-consistently calculated. The ionization rate distribution (production of electron-ion pairs per unit volume per unit time) is displayed in Fig. 2.

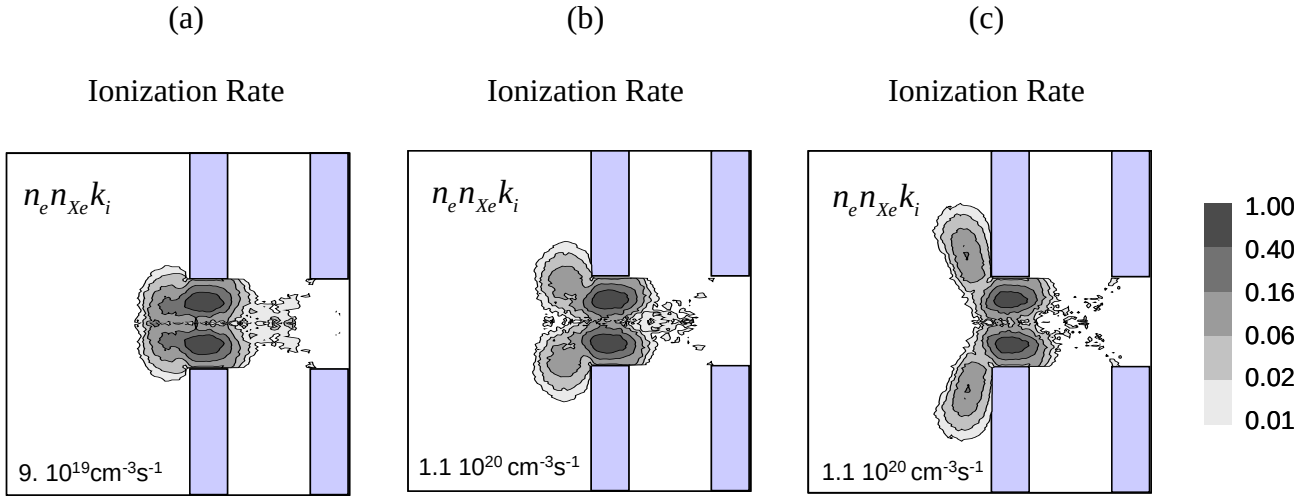

Figure 2: Spatial distribution of the ionization rate in the MHCD of Fig.1 in 30 torr xenon and for 3 values of the electrode voltages: (a) 168 V, 0.046 mA, unit 0.9 10^{20} cm^{-3}.s^{-1}, (b) 173 V, 0.067 mA, unit (log scale, two decades) 1.1 10^{20} cm^{-3}.s^{-1}, (c) 175 V, 0.11 mA, unit 1.1 10^{20} cm^{-3}.s^{-1}. The maximum calculated temperature is respectively: (a) 355 K, (b) 370 K, (c) 380 K. Hybrid model, stepwise ionization not included.

We see on Fig.2 that for lower currents (Fig. 2a), ionization occurs mainly inside the hole. The ionization regions around the surface of the cathode inside the hole slightly overlap. When the current is increased (Figs. 2b and 2c), the ionization region extends outside the hole and starts to cover the back surface of the cathode. This can also be seen on the electric potential contours and ion density distribution displayed in Fig.3 for the same conditions. Under these conditions there is no hollow cathode effect between the sheaths on the back surface of the cathode (such effect transiently occurs in the hollow cathode of a pseudospark discharge[6]) and only the part of the cathode inside the hole contributes to the hollow cathode effect.

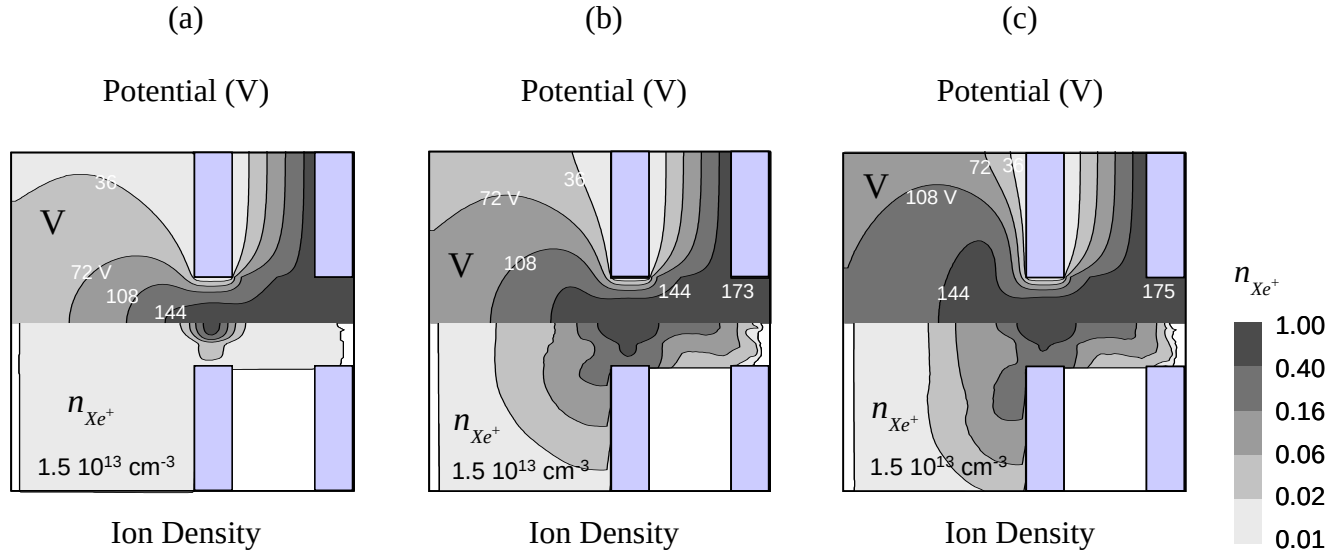

Figure 3: Spatial distribution of the potential (top half) and ion density (bottom half) in the same conditions as Fig.2: MHCD geometry of Fig.1 in 30 torr xenon and for 3 values of the electrode voltage: (a) 168 V, 0.046 mA, (b) 173 V, 0.067 mA, (c) 175 V, 0.11 mA. The unit for the ion density is 1.5 10^{13} cm^{-3} (color bar on the right). The maximum calculated temperature is respectively: (a) 355 K, (b) 370 K, (c) 380 K. Hybrid model, stepwise ionization not included.

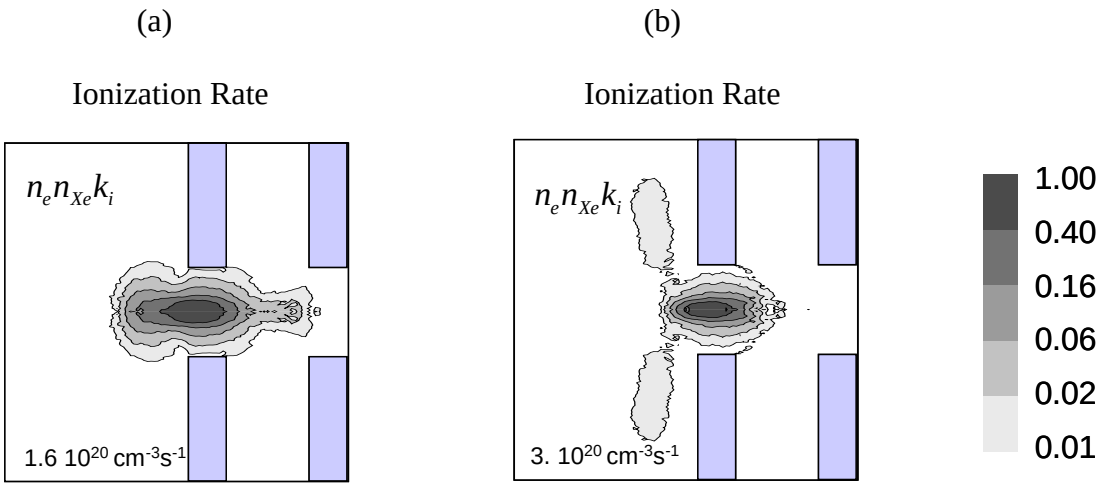

Figure 4: Spatial distribution of the ionization rate in the geometry of Fig. 1 in 15 torr xenon and for 2 values of the electrode voltage: (a) 159 V, 0.035 mA, unit 1.6 10^{20} $cm^{-3}.s^{-1}$ (b) 173 V, 0.072 mA, unit 3 10^{20} $cm^{-3}.s^{-1}$. The maximum calculated temperature is respectively: (a) 355 K, (b) 370 K – Hybrid model, stepwise ionization not included.

Grant 033083 – mid-term report

The hollow cathode effect is more important at lower pressures as can be seen in Fig. 4 which shows the ionization rate distribution at 15 torr for two values of the discharge current. In this case the ionization regions around the sheath inside the cathode hole clearly overlap. As in the previous case, the back part of the cathode does not significantly contribute to the hollow cathode effect. The hollow cathode effect inside the hole does not have dramatic consequences on the current voltage characteristics because of the relatively low voltage (the discharge operates in a "normal" glow regime, i.e. at the minimum voltage) compared for example with pseudospark conditions[6]. However the fact that the current at 30 torr for a voltage of 173 V (see Fig. 2b) is lower than the current at 15 torr for the same voltage (see Fig. 4b) is a clear indication that the hollow cathode effect exists and is more important at 15 torr.

II.2 Gas temperature

In the conditions of a MHCD with dimensions as in Fig. 1 and in a rare gas, it is expected that most of the gas heating occurs in the sheath region by energy transfer from ions to neutral atoms through elastic and charge exchange collisions. Gas heating leads to a decrease in the local neutral density and this may have important consequences on electron energy deposition in the sheath region and therefore on the sheath structure itself.

As mentioned in the Appendix (see section A1.3) there are uncertainties in the self-consistent calculation of the gas temperature. This is because part of the strong ion heating ($j_i.E$) in the sheath is released in the gas through collisions and part is released directed on the cathode, depending on the length of ion and neutral atom collision mean free paths compared with the sheath length[7]. Our model uses a fluid description of ion transport and is not able to accurately predict the part of the ion energy released in the gas. The parameter a (eq. 22 in the appendix) is used to adjust the value of the fractional ion energy dissipated in the sheath and leading to gas heating. In most calculations presented here a is taken to be ¼ .

Figure 5 compares calculations performed with a=¼ and a=1 for a MHCD in xenon at 100 torr (stepwise ionization not included). The current is similar in both cases (~0.5 mA). The calculations show that the maximum temperature is 650 K for a=¼ (Fig. 5c), and 1000 K for a=1 (Fig. 5d). The difference in temperature is not as large as expected (since 4 times more energy is released in the sheath for a=1 one could expect that the temperature increase with respect to ambient temperature be 4 times larger than for a=¼). This is because, due to the temperature increase in the sheath region in the cathode hole, the gas density decreases and the ion current density to the cathode inside the hole decreases (and therefore the power dissipated by ions in the hole region is actually lower for a=1). It is interesting to note that because of the higher temperature in the hole in Fig. 5d (a=1), the plasma expands outside the hole and the sheath covers a larger part of the back surface of the cathode). This can be seen on the ionization rate distributions displayed in Figs. 5c and 5d, and from the potential and ion density distributions shown in Figs. 5a and 5b,

Figures 5c and 5d also confirm that the hollow cathode effect is not really important at 100 torr (the ionization regions around the cathode hole do not significantly overlap). We also see that the ionization region inside the hole is larger for a=1 (Fig. 5d) than for a=¼ because the temperature is higher and the gas density lower for a=1. Note that for a gas temperature of 1000 K, the gas density at 100 torr is the same as the gas density at 30 torr 300 K; from the discussion in section II.1 above one can therefore expect the hollow cathode effect to become important at 100 torr only for gas temperatures above 1000 K.

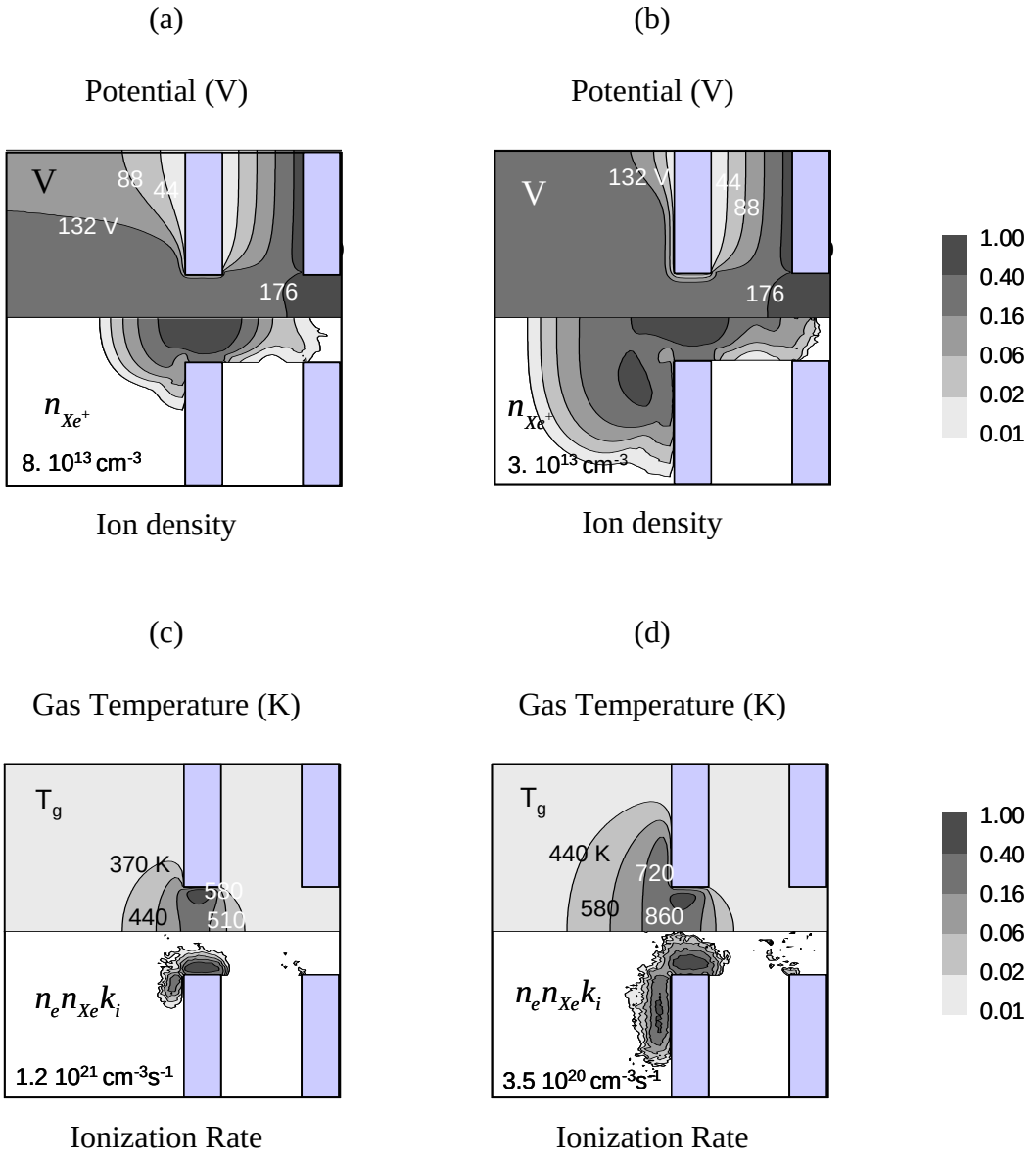

Figure 5: Potential, ion density, gas temperature and ionization rate for a MHCD at 100 torr and for two different assumptions on the gas temperature calculations. (a) and (c): gas heating by ions is described as in eq. (22) in section A1.3 of the appendix (i.e. ¼ of the ion energy is dissipated in the gas, the rest being dissipated on the cathode surface); (b) and (d): all the ion energy is dissipated through collisions in the gas (i.e. a=1 in eq. (22)). Voltage and current are (195 V, 0.52 mA) for (a),(c), and (200 V, 0.5 mA) for (b),(d)

II.3 Hybrid and fluid model

The fluid model cannot describe the hollow cathode effect because the approximations in the electron momentum and energy equations do not allow the description of the fast electrons oscillating between the sheaths. Also, the collision terms (ionization, energy loss frequency, see Appendix 1) in the electron transport equations are obtained by assuming that the electron energy distribution function is completely defined by the electron mean energy, with a shape identical to the energy distribution of an electron swarm under a uniform field. This is obviously not true in the sheath region of a glow discharge where secondary electrons are

accelerated on a short distance by the sheath electric field. Therefore we cannot expect the fluid model to give a very accurate description of the discharge even when the hollow cathode effect is not important. However since the MHCD operates at relatively low voltage, in a "normal" glow discharge regime where the sheath length is not "too short", it is tempting to try using the fully fluid model in these conditions.
Figure 6 displays the gas temperature and ionization rate distributions at 100 torr in xenon, in conditions similar to those of Fig. 5 showing results from the hybrid model (Monte Carlo description of fast electron transport). The current (~0.3 mA) is lower than in the hybrid model (~0.5 mA), and the voltage is higher (~230 V instead of ~200 V). Although the voltage and current obtained in the fully fluid and hybrid models are significantly different, we see that the general conclusions drawn in the last section from the hybrid model could also be deduced from the fully fluid model results. The ionization rate and temperature distributions of Fig. 6 are similar to those of Fig. 5 (the ionization rate is more "localized" in the fluid model because the large energy relaxation length of the fast electrons is not well described in the fully fluid model).

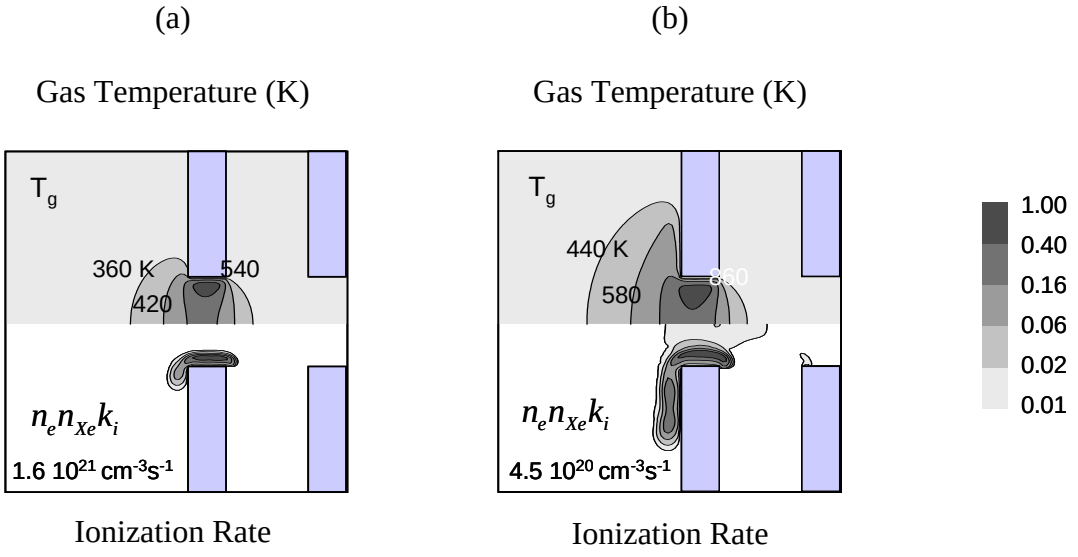

Figure 6: Gas temperature (linear scale) and ionization rate at 100 torr (log scale, 2 decades) for two different assumptions on the gas temperature calculations, as in Fig. 5, but obtained with a fully fluid model of the discharge (i.e. ¼ of the ion energy is dissipated in the gas in Fig. 6a, all the ion energy is dissipated in the gas in Fig. 5b). The voltage and current are (234 V, 0.33 mA) for (a) and (231, 0.34 mA) for (b)

We can conclude that although the fully fluid model is not accurate, it can be useful for a qualitative study of the trends (when the hollow cathode effect is not important).

II.4 Excited species kinetics and stepwise ionisation

All the calculations above assume that all ionization is due to direct electron impact ionization of ground state xenon atoms. This is a non-realistic assumption, especially at high pressure, but the results above are useful to clarify the hollow cathode and gas temperature effects. The calculations including the metastable atoms described below show that stepwise ionization plays an important role in the MHCD conditions. The electrons accelerated in the sheaths release their energy in the glow through inelastic collisions. The metastable atom

density builds up in the negative glow and ionization of the metastable atoms by electrons in the bulk of the distribution becomes possible.
The calculations in this section are performed with the fully fluid model.
Figure 7 shows the contribution of direct and stepwise ionization (Fig. 7a) in a MHCD in Xe at 100 torr, and the distribution of potential and total electron excitation (Fig. 7b).

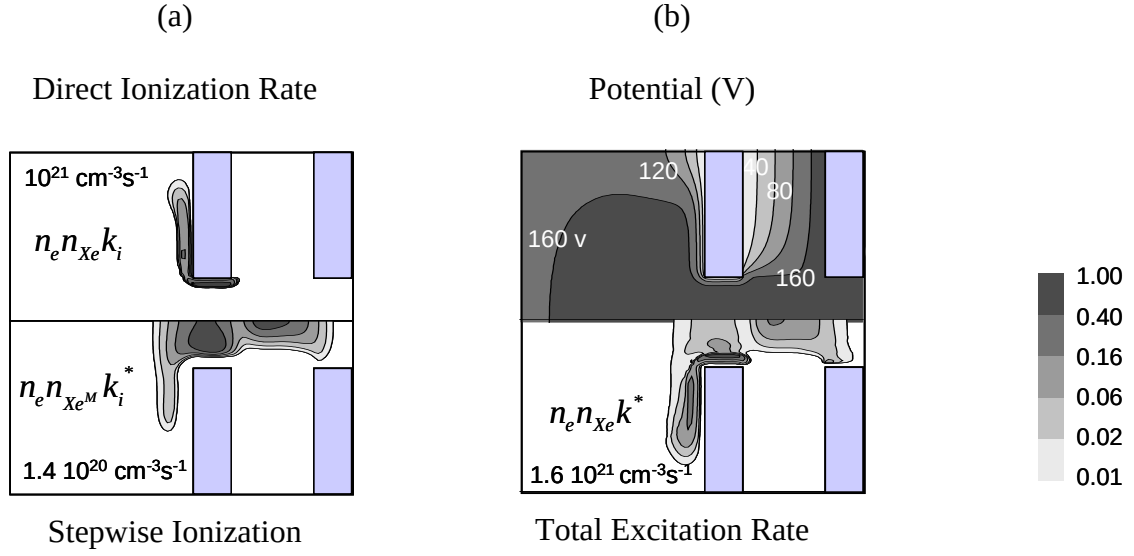

Figure 7: (a) Total electron source term and stepwise ionization (log scale, 2 orders of magnitude), (b) electric potential (linear scale) and total excitation rate in a MHCD at 100 torr in xenon (excited species kinetics and gas temperature calculation included) (log scale, 2 orders of magnitude). Voltage and current: (190 V, 0.54 mA)

We see in Fig. 7 that the maximum of stepwise ionization is about 15% of of the maximum of direct ionization and that the total stepwise ionization is dominant in regions further from the cathode sheath (i.e. in regions where the mean electron energy is lower).

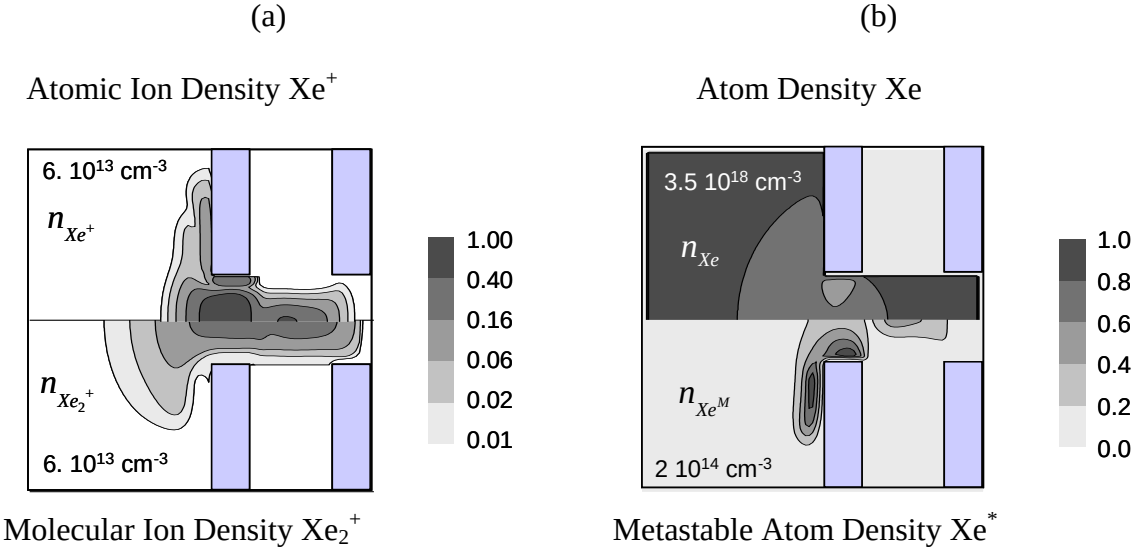

Figure 8: (a) atomic and molecular ion densities (log scale) , and (b) atom and metastable atom densities (linear scale) in the conditions of Fig. 7 (MHCD in Xe at 100 torr with selfconsistent calculation of gas temperature and stepwise ionization); Voltage and current: : (190 V, 0.54 mA)

The atomic and molecular ion densities as well as the total and metastable atom densities are displayed in Fig. 8 for the same conditions as Fig. 7. The plasma density reaches values close to 10^{14} cm^{-3} in the cathode hole. The maximum density of molecular ions is 1.4 10^{13} cm^{-3} compared with 6. 10^{13} cm^{-3} for the density of atomic.
The minimum of the xenon atom density (Fig. 8b) in the cathode hole is due to the temperature increase. The metastable atom density is large and on the order of 10^{14} cm^{-3} in the glow region which extends a few 10s of microns beyond the sheath. The metastable atom density also increases from the end of the negative glow inside the hole toward the anode (see also the total excitation rate in Fig. 7b). This region is similar to a short positive column.

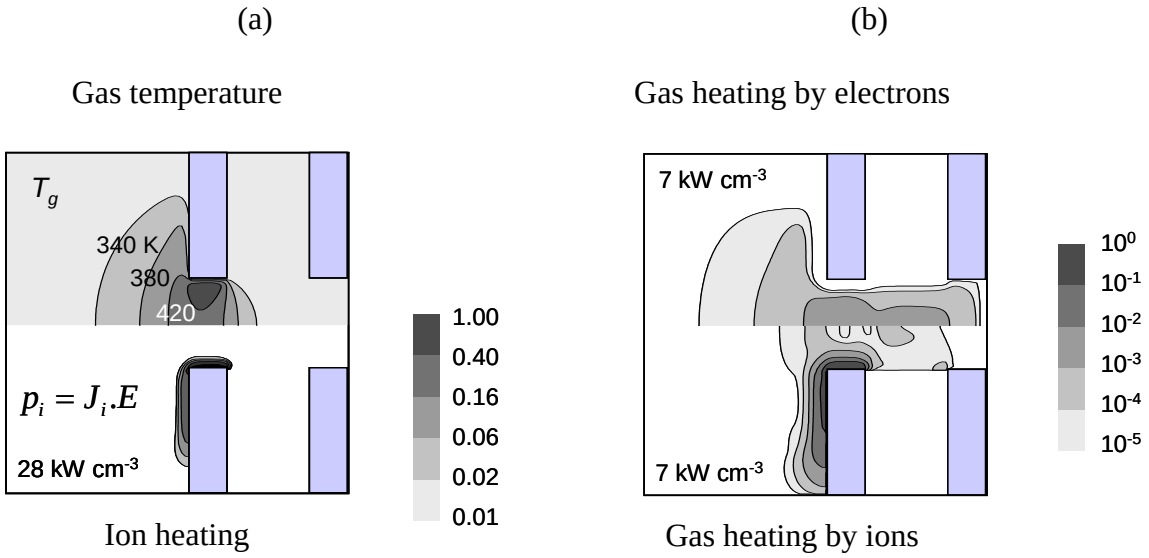

Figure 9: (a) Gas temperature (linear scale) and ion heating (log scale 2 decades) , and (b) gas heating by electrons and ions (log scale 5 decades) in the conditions of Figs. 7 & 8 (MHCD in Xe at 100 torr); Voltage and current: (190 V, 0.54 mA)

Figure 9 shows the ion heating ($J_i.E$) distribution and the gas temperature contours (Fig. 9a) and the contribution of electrons and ions to gas heating (Fig. 9b). Note that the power dissipated into ion heating in the sheath reaches values as high as several kW/cm^{-3}. The gas temperature peak is about 500 K. Since we assume that ¼ of the ion energy is converted into gas heating (eq. 22 in the Appendix) the gas heating due to ion power deposition shown in Fig. 9b is 4 times less than the ion heating (J_i.E). The gas heating in the bulk plasma due to electron-atom elastic collisions also represented in Fig. 9b is less than three orders of magnitude lower than the heating due to ions in the sheaths (the maximum of the calculated gas heating by electrons is about 20 W.cm^{-3}, vs 7 kW.cm^{-3} for ions). Note that 5 orders of magnitudes are represented in the gas heating of Fig. 9b while only two orders of magnitude are displayed in the ion heating plot of Fig. 9a.

In the plasma column, the power deposition by electrons is (eq. 21 of the Appendix) $n_e \nu_m \frac{2m}{M} \varepsilon_e$. For $n_e \sim 2.10^{13}$ cm^{-3}, $\nu_m \sim 10^{11}$ s^{-1} at 100 torr, $m/M \sim 10^{-5}$, and ε_e~3eV we get $n_e \nu_m \frac{2m}{M} \varepsilon_e \sim 10^{20}$ $eV.cm^{-3}.s^{-1} \sim 20$ $W.cm^{-3}$ in agreement with the results shown in Fig. 5b.

Note finally that the presence of metastable atoms and stepwise ionization leads to a decrease of the operating voltage for a given current: the current in the case of Figs. 7-9 are is 0.5 A for an applied voltage of 190 V, to be compared with 231 V for 0.34 mA in the case of Fig. 6b (both cases have been obtained with the fully fluid model).

III. DISCUSSION

III.1 Basic discharge properties

Figure 10 the different current-voltage characteristics obtained with the model for various pressures and with the hybrid and fluid models.

A general trend is that the slope of the V-I curve is larger at lower currents and becomes almost flat at higher current for higher pressure (and when metastable are included in the simulation). The first slope corresponds to a situation where the discharge occurs mainly inside the hole and the current increases for increasing voltage. This is equivalent the "abnormal regime" of the discharge inside the hole. When the current and voltage become large enough the discharge moves to the back surface of the cathode and quickly spreads with increasing current while the voltage no longer increases or increases slowly. This part of the characteristics corresponds to a "normal regime" of the glow discharge where most of the current is drawn through the back surface of the cathode.

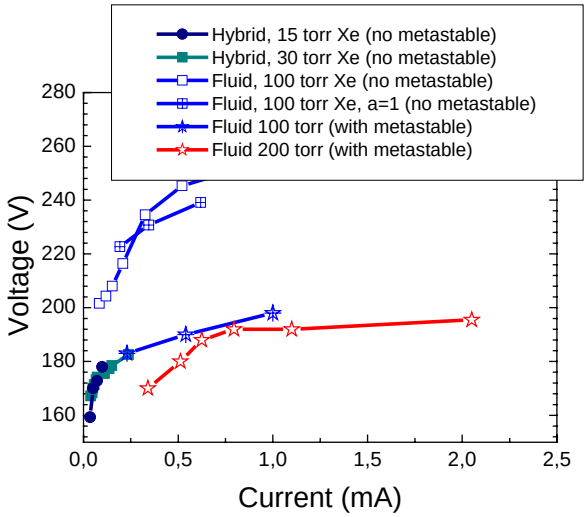

Figure 10: Current-voltage characteristics for different conditions with the hybrid and fully fluid models, with and without metastable included. In one case (indicated a=1), the calculations have been performed assuming that all the ion energy is deposited in the sheaths (see eq. [22] in the appendix)

The experimental results of Shi et al. shown in Fig. 11 show that the measured current-voltage characteristics exhibit a maximum in the voltage at low currents. Below this maximum the slope of the V-I curve is large; after the maximum in voltage the voltage drops abruptly and the voltage is almost constant when the current increases (after a region of

negative slope of the V-I characteristics). The region of negative slope after the peak voltage has been attributed to a hollow cathode effect by Schoenbach et al.. However, the simulation results do not confirm this interpretation. The models do not reproduce the maximum in voltage but predict an abrupt change of slope in the V-I characteristics at low currents (see especially the V-I curve of Fig. 10 for p=200 torr). As said above this change of slope marks the beginning of the extension of the plasma on the back surface of the cathode.

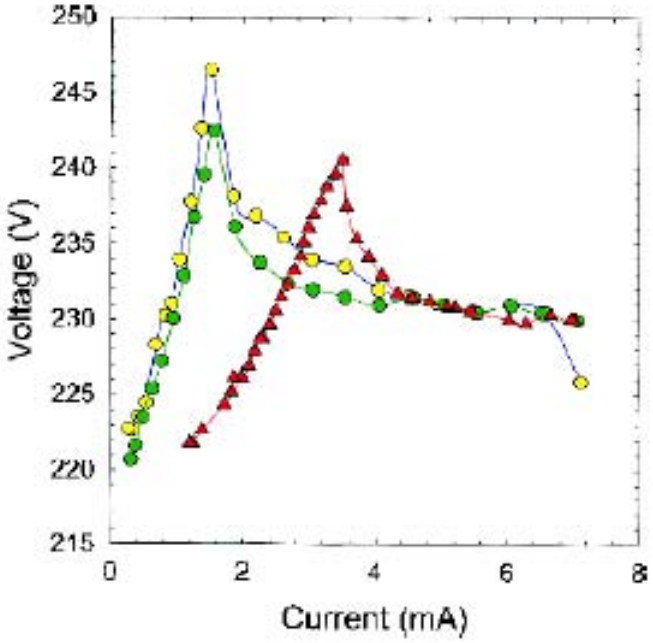

Figure 11: Current–voltage characteristics of each of the two hollow cathode discharges (circles) in a two-hole configuration and current–voltage characteristic of the two-hole discharge array (triangles). Argon pressure of 400 torr, hole diameter 100 μm, mica dielectric 200 μm. (after Shi et al.[9])

Another interesting feature appearing in the experimental results (Moselhy and Schoenbach, personal communication) is the fact that for a given current, the operating voltage decreases when the pressure increases. This is surprising since one could expect that the sheath voltage does not change while the positive column voltage increases when the pressure increases, leading to an increase of the total voltage. The observed decrease of the operating voltage with increasing pressure can probably be attributed to the effect of the metastable and stepwise ionization. The contribution of stepwise ionization increases with pressure and does not follow the basic glow discharge scaling laws. The models give similar trends (compare the 100 torr and 200 torr V-I characteristics in Fig. 10) : the operating voltage at 200 torr is lower than at 100 torr when stepwise ionization is included. We did not perform simulations for pressure above 200 torr, because it would have been necessary, in order to keep constant the numerical accuracy, to increase the number of grid points linearly with pressure (we used a 100x100 uniform grid at 100 torr, and a 200x200 uniform grid at 200 torr). Non uniform grids will be used in future work.

III.2 Power deposition, temperature and stability

As mentioned above, the discharge is located inside the hole only at low currents. Above typically 1 mA, the discharge develops outside the hole, along the back surface of the cathode. For example, at 200 torr and for a current of 2 mA, the discharge entirely covers the 0.5 mm radius of the back surface of the cathode (at 100 torr, the discharge covers the

cathode surface when the current reaches 1 mA). Figure 12 shows the spatial distributions of electron density and metastable atom density at 200 torr and for the 6 points of the V-I curve of Fig. 10 (star symbols). We see that above 0.6 mA the discharge starts to cover the back surface of the cathode. At 2 mA, the 1 mm radius of the cathode in the simulation is completely covered by the plasma as can be seen in Fig. 12. Assuming that the current density stays constant when the discharge spreads on the back surface, one can expect that the radius of the discharge increases as the square root of the current. The discharge diameter on the back surface of the cathode is about 1 mm at 2 mA and should therefore be on the order of 2.5 mm for a current of 10 mA at 200 torr. These numbers seem consistent with the experiments[9]. Note however that the experimental results show that the discharge may not be homogenous on the back surface of the cathode for large currents[9].

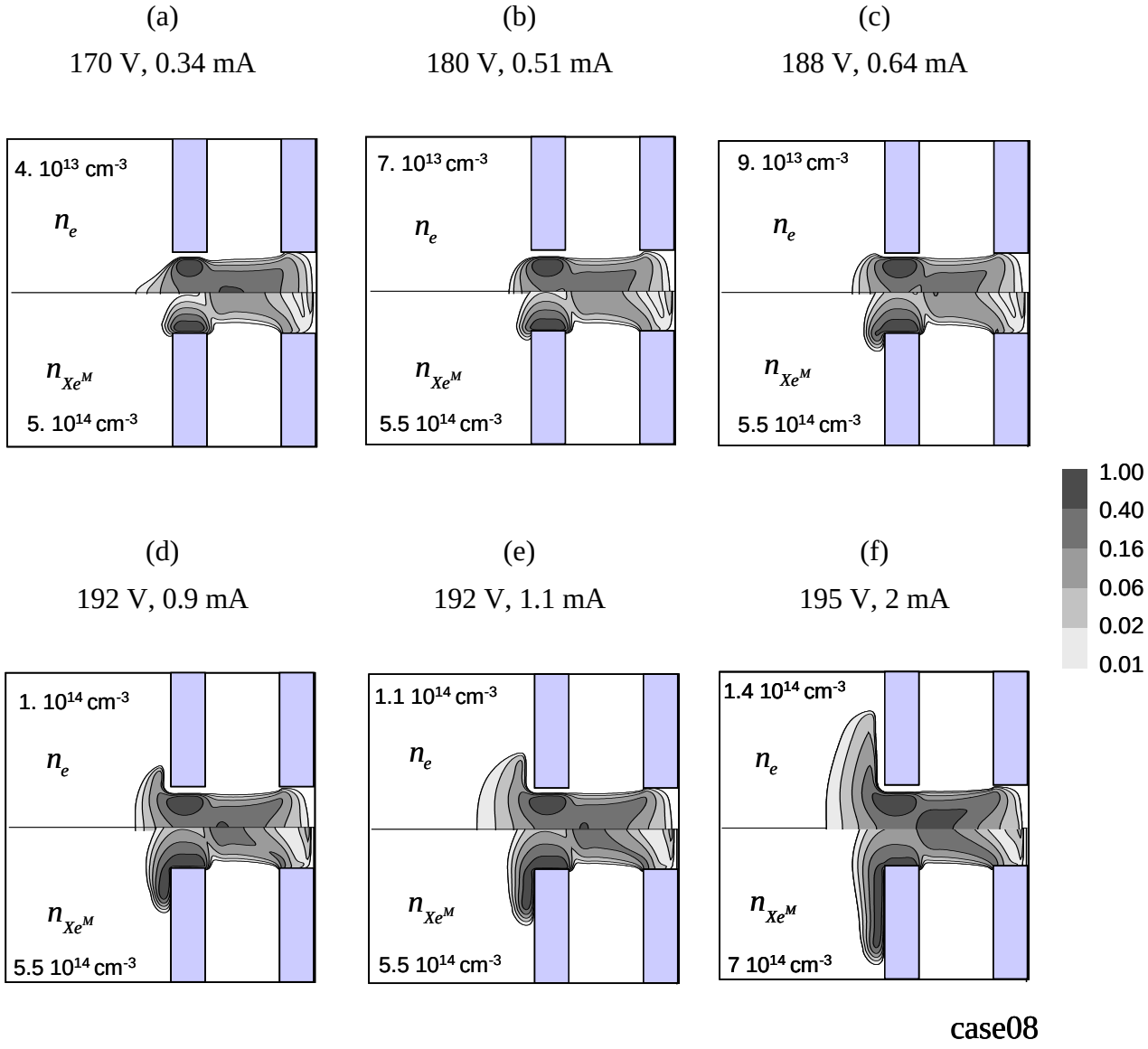

Figure 12: Distribution of electron density (top half of each figure) and metastable atom density for a MHCD (bottom half of each figure) at 200 torr and for different points on the V-I characteristics (red stars on the V-I curve of Fig. 10). The unit is indicated on each half figure. Log scale, 2 decades (color bars on the right)

The results of Fig. 12 show that the power deposited in the hole region does not actually increase significantly when the current increases, provided that the discharge can extend on the back surface of the cathode. This is confirmed by the plot of the maximum gas temperature in the hole as a function of the discharge current in Fig. 13. The gas temperature increases relatively slowly with increasing current above 0.6 mA.

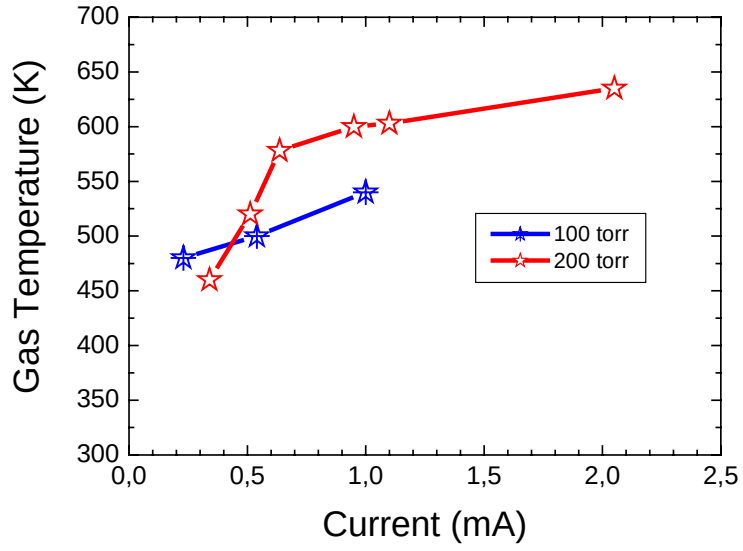

Figure 13: Maximum calculated gas temperature in the hole as a function of discharge current for 100 torr and 200 torr discharges in xenon (correspond to the data with same symbols on the V-I curves of Fig. 10).

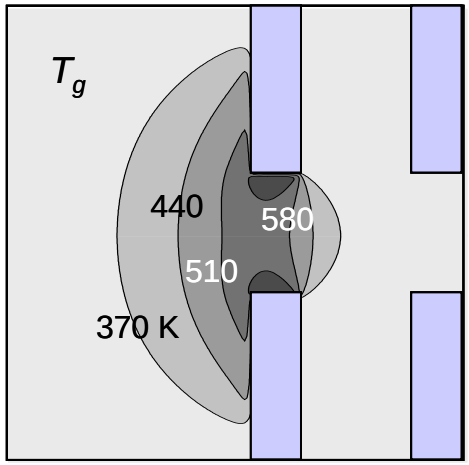

Figure 14: Calculated gas temperature distribution in the MHCD at 200 torr in xenon for voltage and current of 195 V, 2 mA. The maximum temperature is 635 K.

Note finally that, as shown in Fig. 14, the gas temperature in the sheath region above the back surface of the cathode is significantly lower than the gas temperature inside the hole and the risk of temperature instability in this region is limited. In the conditions considered here, the power deposition by electrons is too small to significantly contribute to gas heating in the plasma column confined by the dielectric layer. This would obviously be different in a molecular gas or for higher currents or pressures.

IV. CONCLUSIONS

From the preliminary results presented in this report we can draw the following conclusions:

- the hollow cathode effect due to electron oscillations between sheaths is unlikely to play an important role in the conditions of the MHCDs of Prof Schoenbach's group (unless the gas temperature in the cathode hole reaches values larger than 1000 K at 100 torr, or even larger at higher pressure)
- the gas temperature is maximum in the cathode hole region due to the large energy deposition by ions and because of the hole geometry. Although more work is needed to obtain better estimations of the gas temperature we can reasonably conclude from the calculations that the gas temperature in the cathode hole region can reach 600 to 1000 K for a current and voltage of 1 mA and 200 V at 100 torr in xenon. A temperature increase in the cathode hole induces a decrease in the gas density which leads to a decrease of the current collected by the part of the cathode inside the hole and prevents a further increase in temperature. This effect controls the temperature in the hole and helps preventing a glow to arc transition. The temperature in the hole only increases slowly with increasing current provided the discharge can spread on the back surface of the cathode. More work is needed to estimate the gas temperature for higher current and higher pressure conditions (experiments show that the MHCD in xenon can be operated up to 10 mA for pressure larger than 500 torr). The model does not provide information on the temperature of the cathode surface.
- The current voltage characteristics of the MHCD is rather flat as long as the discharge can spread along the back surface of the cathode. The extension of the discharge along the back surface increases with current. Values of the current and discharge diameter on the cathode surface are in agreement with the experiments in the pressure range considered in this report (100-200 torr)
- stepwise ionization contributes in a non negligible way to the total ionization in the sheath and is dominant in the plasma bulk. Stepwise ionization is probably responsible for the decrease of the operating voltage at constant current which has been observed in the experiments.
- Further work will be in the direction of: better estimation of the gas temperature, parametric study of the influence of the assumptions of the excited species model, possible effect of secondary emission due to metastable of photons, extension of the model to higher pressure situations (numerical questions to solve), consequences of using fully fluid instead of hybrid model (much more time consuming at higher pressure), more detailed comparisons with experiments, investigation of pulsed regime.

REFERENCES

[1] KH Schoenbach, A. El-Habachi, W. Shi, and M. Ciocca, *High pressure hollow cathode discharges*, Plasma Sources Sci. Technol. **6**, 468 (1997)

[2] KH Schoenbach, A. El-Habachi, MM Moselhy, W Shi, and RH Stark, *Microhollow cathode discharge excimer lamps*, Phys. Plasmas **7**, 286 (2000).

[3] RH Stark and KH Schoenbach, *Direct high pressure glow discharges*, J. Appl. Phys. **85**, 2075 (1999)

[4] RH Stark and KH Schoenbach, *Electron heating in atmospheric glow discharges*, J. Appl. Phys. **89**, 3568 (2001)

[5] EE Kunhardt, *Generation of large volume, atmospheric-pressure, non-equilibrium plasmas*, IEEE Trans Plasma Sci. **28**, 189 (2000)

[6] J.P. Boeuf and L.C. Pitchford, *Pseudospark discharges via computer simulation*, IEEE Trans. Plasma Sci. **19**, 226 (1991)

[7] I. Revel, L. Pitchford, J.P. Boeuf, *Calculated gas temperature profiles in argon glow discharges*, J. Appl. Phys. **88**, 2234 (2000)

[8] M. Moselhy, W. Shi, R. Stark, A flat glow discharge excimer radiation source, IEEE Trans. Plasma Sci. **30**, 198 (2002)

[9] W. Shi, R. Stark, and K. Schoenbach, Parallel Operation of Microhollow Cathode Discharges, IEEE Trans. Plasma Sci. **27**, 16 (199)

[10] J. P. Boeuf et L. C. Pitchford, *Two-dimensional model of a capacitively coupled rf discharges and comparisons with experiments in the Gaseous Electronics Conference reference reactor*, Phys Rev E **51,** 1376 (1995).

[11]G.J.M. Hagelaar and G.M.W. Kroesen, *Speeding up fluid models for gas discharges by implicit treatment of the electron energy source term*, J. Comp. Phys. **159**, 1 (2000)

[12] L.C. Pitchford, J. Kang, C. Punset, and J.P. Boeuf, *Calculated characteristics of rf plasma display panel cells including the influence of xenon metastables*, J. Appl. Phys. **92**, 6990 (2002)

[13] VV Serikov and K. Nanbu, *The analysis of background gas heating in direct current sputtering discharges via particle simulation*, J. Appl. Phys **82**, 5948 (1997)

[14] SS Sahzin and VV Serikov, *Rarefied gas flows : hydrodynamic versus Monte Carlo modelling*, Planet. Space Sci. **45**, 361 (1997)

ANNEX A1: MODEL DESCRIPTION

A1.1 Hybrid fluid-Monte Carlo model and fully fluid model

In this section we describe the basic equations of the model when the only ionization process taken into account is direct electron impact ionization of ground stated atoms and only atomic ions are considered.
The model is based on the following set of equations:

$$\frac{\partial n_e}{\partial t} + \nabla.\mathbf{\Gamma}_e = S_e \qquad [1]$$

$$\frac{\partial n_i}{\partial t} + \nabla.\mathbf{\Gamma}_i = S_i \qquad [2]$$

$$\Delta V = -\frac{e}{\varepsilon_0}\left[n_i - n_e\right] \qquad [3]$$

where n_e and n_i, are respectively the electron and ion number densities, Γ_e and Γ_i the electron and ion flux, V the electric potential, S_e and S_i are the electron and ion production rates. [1], [2], are the electron and positive ion continuity equations, and [3] is Poisson's equation.
The charged particle fluxes are approximated by drift-diffusion equations of the form:

$$\mathbf{\Gamma}_e = -n_e\mu_e\boldsymbol{E} - D_e\nabla n_e \qquad [4]$$

$$\mathbf{\Gamma}_i = n_i\mu_i\boldsymbol{E} - D_i\nabla n_i \qquad [5]$$

where $\mu_{e,i}$ and $D_{e,i}$ are the electron and ion mobility and diffusion coefficients. The ion mobility is supposed to depend on the local electric field and the ion diffusion coefficient is taken as a constant and such that $D_i / \mu_i \approx 0.1$ V. This value of D_i is rather arbitrary but ion diffusion does not play a crucial role in this discharges and moreover, numerical diffusion is larger than ion diffusion in most fluid discharge models. The treatment of electron mobility and diffusion is different in the hybrid model and in the fully fluid model and is described in the corresponding sub-sections below.
The boundary condition for the electron flux at the cathode is

$$\mathbf{\Gamma}_{e,out} = \gamma\,\mathbf{\Gamma}_{i,in} \qquad [6]$$

where γ is the secondary electron emission coefficient, $\mathbf{\Gamma}_{e,out}$ is the flux of secondary electrons out of the cathode, and $\mathbf{\Gamma}_{i,in}$ the flux of ions to the cathode. The secondary electron emission is supposed to be constant and equal to 0.05 in the calculations presented here.
The charged particle flux toward a boundary (electrode or dielectric) is given by:

$$\mathbf{\Gamma}_{in} = \pm an\mu E + \frac{1}{4}n\mathrm{v}_{th} \qquad [7]$$

where a is 1 if the particle drift velocity is directed toward the boundary and 0 otherwise; v_{th} is the particle thermal velocity.
If we assume that most of the ionization is due to electron impact ionization of ground state atoms, the source terms of the electron and ion continuity equations [1] and [2] are written as:

$$S_e = S_i = S = n_e N k_i \qquad [8]$$

where N is the xenon atom density and k_i the electron impact ionization rate of the xenon atoms. In the conditions of the MHCDs, the cathode fall region plays an important role, and a large part of the total ionization is due to secondary electrons emitted at the cathode and accelerated in the sheaths.

We have considered two ways of calculating *S*. The first one is based on a Monte Carlo simulation of the trajectories of electrons emitted by the cathode (hybrid model), and the second one uses a fluid energy equation for the electrons.

Hybrid Model

In the hybrid model the ionization source term is deduced from a Monte Carlo simulation:

$S \equiv S_{MC}$

The electrons emitted by the cathode are followed until their energy does not allow them to undergo any more ionization event. Knowing the flux of secondary electrons from the fluid model, this simulation provides the spatial distribution of the source term S. The charged particle densities and electric field are obtained from equations [1]-[5]. At each call, the secondary electrons are treated in a quasi-steady state way. Between two Monte Carlo calls, the fluid equations are solved with the same source term (which can be optionally weighted by the time dependent ion current to the cathode) for a given time interval. The time interval between two Monte Carlo calls can be adjusted in several ways: a maximum relative variations of the calculated current and voltage can be prescribed (typically in the 10% range at the beginning of the simulation and on the order of 1% when reaching steady state); a maximum time interval or number of time steps between Monte Carlo calls can also be prescribed. The number of electrons simulated at each Monte Carlo call can be relatively small (on the order of a few 100). The statistical noise is reduced by under-relaxing the source terms between successive Monte Carlo calls. These different parameters controlling the coupling of the fluid model and the Monte Carlo simulation are adjusted and optimized in an empirical way depending on the conditions.

In the hybrid model used here the electron mobility is supposed to depend on the local electric field and the electron diffusion coefficient is fixed in such a way that:

$D_e / \mu_e = 2$ V

Fully fluid model

Another less accurate but less time consuming way of calculating the source term is to add an energy equation to the electron continuity and drift-diffusion equations. Although this approach is not as the hybrid model it can be useful to provide general trends. Also, the transient evolution of the discharge toward steady state can be very time consuming in the hybrid model, and the fully fluid model can be first used to approach steady state.

The electron energy equation has the following form:

$$\frac{\partial n_e \varepsilon_e}{\partial t} + \nabla.\mathbf{\Gamma}_{\varepsilon,e} = S_{\varepsilon,e} \qquad [9]$$

where ε_e is the electron mean energy, $\mathbf{\Gamma}_{\varepsilon,e}$ an energy flux, and $S_{\varepsilon,e}$ the energy source term including electron heating by the electric field, and energy losses due to collisions.

Using classical approximations, the energy flux defined above is written:

$$\nabla.\mathbf{\Gamma}_{\varepsilon,e} = -\frac{5}{3} n_e \varepsilon_e \mu_e \boldsymbol{E} - \frac{5}{3} D_e \nabla\left(n_e \varepsilon_e\right) \qquad [10]$$

and the electron energy source term is given by:

$$S_{\varepsilon,e} = -e\mathbf{\Gamma}_e.\boldsymbol{E} - n_e L \qquad [11]$$

where the energy loss term *L* is supposed to depend only on the mean electron energy.

The electron diffusion coefficient in the equations above is supposed to be given by the Einstein relation:

$$\frac{D_e}{\mu_e} = \frac{2}{3}\frac{\varepsilon_e}{e} \qquad [12]$$

The form of $L(\varepsilon_e)$ in equation [11] is obtained by writing the energy balance for an electron swarm at steady state under a uniform electric field. As a first approximation, at steady state and under uniform conditions, we have $S_{\varepsilon,e} \approx 0$ and therefore $L \approx e\mu_e E^2$ (knowing the variations of mean electron energy ε_e as a function of E/N under uniform field conditions, this loss term can be tabulated as a function ε_e). A more accurate estimation of L is obtained by noting that in a uniform field and under steady state conditions the mean energy or drift velocity is constant but the density gradient are not zero (because of ionization). At steady state under a uniform electric field we have from continuity equation: $|\nabla.n_e| = \alpha n_e$ where α is the ionization coefficient. Using equations [4], [9] and [10] under these conditions, together with the Einstein relation, we obtain a more consistent relation for $L(\varepsilon_e)$:

$$L(\varepsilon_e) = e\mu_e E^2 \left[1 - \frac{7}{3}\frac{\alpha\varepsilon_e}{eE} + \frac{10}{9}\left(\frac{\alpha\varepsilon_e}{eE}\right)^2 \right] \qquad [13]$$

This correction is not negligible when ionization is important and using this form of $L(\varepsilon_e)$ ensures that the fluid model provides at least consistent values of the breakdown voltage under uniform or quasi-uniform electric field conditions. For each value of E/N, the mean electron energy and the right hand side of equation [11] can be calculated by using a Boltzmann equation solver. This provides tabulated values of $L(\varepsilon_e)$.

Knowing the electron mean energy at a given location and time, the ionization rate in the continuity equations [1] and [2] is obtained by assuming that this rate depends on the mean energy with the same functional form as under uniform field conditions. In the same way as $L(\varepsilon_e)$, $k_i(\varepsilon_e)$ is tabulated by using a Boltzmann equation solver which provides both k_i and ε_e for a series of values of *E/N*.

The principles of the fully fluid model described above and the numerical technique are similar to those of the model used in Ref. [10] for rf glow discharges. The numerical method has been improved to allow for larger time steps in the integration of the energy equation, based on the ideas discussed in Ref. [11].

A1.2 Excited species kinetics

To study in a semi-quantitative way the possible contribution of the excited species to the overall ionization and the possible contribution of molecular ion formation and recombination to the overall electron loss, a very simple model has been used. This excited species kinetics model includes the following reactions:

$Xe + e \rightarrow Xe^+ + 2e$	*(1) ground state ionization*	k_i from Boltzmann eq.
$Xe + e \rightarrow Xe^* + e$	*(2) Excited state production*	k^* from Boltzmann eq.
$Xe^* + e \rightarrow Xe^+ + e$	*(3) Excited state ionization*	k_i^* from Boltzmann eq.
$Xe^* + Xe^* \rightarrow Xe + Xe^+$	*(4) Associative ionization*	k_{ia} $5.\,10^{-10}$ cm^3s^{-1}
$Xe^* + 2Xe \rightarrow Xe_2^*$	*(5) Excimer formation*	k_{3B} 10^{-31} cm^6s^{-1}
$Xe^R \rightarrow Xe + h\nu$	*(6) Resonant emission*	ν_r 10^6 s^{-1}
$Xe^+ + 2Xe \rightarrow Xe_2^+ + Xe$	*(7) Ion conversion*	k_c $2.5\,10^{-31}$ cm^6s^{-1}
$Xe_2^+ + e \rightarrow 2Xe$	*(8) El-molecular ion recomb.*	r 10^{-7} $T_e^{-1/2}$

Table I: Simple model of the excited species kinetics in xenon, Xe^* represents xenon atoms in the resonant or metastable states

The species considered in the simulation are: electrons, atomic ions, molecular ions and metastable atoms. Their densities are noted respectively: n_e, $n_{X_e^+}$, $n_{Xe_2^+}$ and $n_{X_e^M}$. The resonant state density is noted $n_{X_e^R}$ and the ratio of the resonant to metastable density is noted α: $\alpha = \frac{n_{X_e^R}}{n_{X_e^M}}$. The sum of the resonant and metastable state densities is noted $n_{X_e^*} = n_{X_e^M} + n_{X_e^R}$

The basic assumptions of the excited species kinetics model are the following and are consistent with Table I above:

- electron impact excitation of xenon ground state atoms populate the resonant state of xenon, the metastable state, and upper levels. We assume that excitation to the upper levels instantaneously goes back to the metastable and resonant states through cascading and spontaneous emission. The global rate of production of excited states by electron impact from the ground state is noted k^*.
- we assume that the density ratio of the resonant to metastable states is constant: $\alpha = \frac{n_{X_e^R}}{n_{X_e^M}} = constant$ (this is a reasonable assumption if there is a strong collisional coupling between the two states which are separated by about 0.1 eV) .
- we sum the rate equations for the resonant and metastable states; the production rate in this equation is therefore $n_e n_{X_e} k^*$; the loss term includes: ionization by electron impact (reaction (3), rate k_i^*), associative ionization (reaction (4), rate k_{ia}) , three body collisions leading to excimer formation (reaction (5), rate k_{3B}) , emission from the resonant state (reaction (6), frequency ν_r). We assume that the rates of reactions (3), (4), and (5) are the same for the resonant and metastable states.
- Atomic ions are converted into molecular ions through reaction (7) (rate *kc*). Molecular ions can recombine with electrons (reaction (8), recombination coefficient *r*).

The source terms of the electron, atomic and molecular ions continuity equations are therefore written respectively:

$$S_e = n_e n_{X_e} k_i + n_e n_{X_e^*} k_i^* + n_{X_e^*}{}^2 k_{ia} - r n_e n_{Xe_2^+} \quad [14]$$

$$S_{Xe^+} = n_e n_{X_e} k_i + n_e n_{X_e^*} k_i^* + n_{X_e^*}{}^2 k_{ia} - n_{Xe}{}^2 n_{Xe^+} k_c \quad [15]$$

$$S_{Xe_2^+} = n_{X_e}{}^2 n_{Xe^+} k_c - r n_e n_{Xe_2^+} \quad [16]$$

k_i and k_i* are the direct and stepwise ionization rates, k_{ia} is the rate for associative ionization, k_c is the rate of conversion of atomic ions to molecular ions, *r* is the electron-molecular ion recombination coefficient, and n_{Xe} and n_{Xe^*} are respectively the atom and metastable number densities.

The density n_{Xe^*} of Xe^* atoms (sum of metastable and resonant state densities) is obtained from the following continuity equation:

$$\frac{\partial n_{Xe^*}}{\partial t} - D\Delta n_{Xe^*} = S_{Xe^*}$$

where *D* is a diffusion coefficient and S_{Xe^*} is given by:

$$S_{n_{Xe^*}} = n_e n_{X_e} k^* - n_e n_{X_e^*} k_i^* - n_{X_e^*}{}^2 k_{ia} - n_{X_e^*} n_{X_e}{}^2 k_{3B} - \nu_r n_{X_e^R} \quad [17]$$

We used a numerical value of 100 torr.cm^2/s for *pD*.

Again, in this simplified model, k^* is the sum of the electron impact excitation rates from the ground state for all excited states of xenon (we assume that the upper excited states quickly cascade to the metastable state). The loss due to photon emission by the resonant state of xenon is represented by the last term of equation [17]. The loss frequency ν_r in equation [1] is the inverse of the effective lifetime of the resonant state and is taken to be 10^6, which is coherent with the Holtstein theory for dimensions in the 100 μm range.
Equation [17] can be slightly transformed to obtain an equation for the metastable atom density $n_{X_e^M}$:

$$\frac{\partial n_{Xe^M}}{\partial t} - D\Delta n_{Xe^M} = \frac{1}{1+\alpha} n_e n_{X_e} k^* - n_e n_{X_e^M} k_i^* - (1+\alpha) n_{X_e^M}{}^2 k_{ia} - n_{X_e^M} n_{X_e}{}^2 k_{3B} - \frac{\alpha}{1+\alpha} \nu_r n_{X_e^M} \qquad [18]$$

The ratio of resonant to metastable density α depends on the details of the kinetics between the xenon excited states and it is very difficult to have a precise estimation of this ratio even with more sophisticated models[12]. We therefore chose to consider α as an adjustable parameter and its value has been varied between 0.1 and 1 in the simulations.
Since some time constant in the metastable equation may be quite long (eg diffusion time), the metastable rate equation above can be solved with a larger time step as the rest of the model (for dc discharge simulations). We used a time step ten times larger for equation [18] than for the charged particle transport equations in the results presented here.

Finally, depending on the model (fluid or hybrid), the excitation and ionization rates k^*, k_i, and k_i^* are either tabulated (as a function of E/N), or obtained from the Monte Carlo simulation.

A1.3 Gas temperature

The gas temperature is obtained from the heat equation (gas flow is not taken into account):

$$\frac{\partial \rho c_v T_g}{\partial t} - \nabla.\kappa \nabla T_g = H \qquad [19]$$

where T_g is the gas temperature, H the power deposited into gas heating by the plasma, and κ the thermal conductivity of the gas (which is relatively low in xenon and approximately equal to 6. 10^{-3} W K^{-1} m^{-1}).
Gas heating may be due either to power deposition by ions in the sheath region (elastic and charge exchange collisions) or by electrons in the plasma column (elastic collisions and, in the case of molecular gases, vibrational excitation followed by vibration-translation energy conversion). In the case of a MHCD in xenon, the power deposition by ions in the sheath is likely to play the dominant role in gas heating. Let us note H_e and H_i the electron and ion contributions to gas heating:

$$H = H_e + H_i \qquad [20]$$

The heating due to electrons can be written as:

$$H_e = n_e \nu_m \frac{2m}{M} \varepsilon_e \qquad [21]$$

where ν_m is the electron-neutral momentum transfer frequency, m and M are the electron and neutral atom masses, and ε_e the mean electron energy.
The ion heating in the sheath is more difficult to estimate because 1) a large part of the ion energy can be released on the cathode and not in the gas, and, 2) charge exchange collisions

lead to the generation of fast neutral atoms which can in turn release their energy by collisions in the gas or on the cathode.
In this first approach we consider that a given, fixed fraction of the ion heating is converted into gas heating, the rest being deposited on the cathode:

$$H_i = a\, \boldsymbol{j}_i.\boldsymbol{E} \qquad [22]$$

where a is a constant parameter (supposed to be ¼ in the calculations reported here).
To solve the heat equation we need to specify the boundary conditions on the electrode and dielectric surfaces. In the calculations reported here, we assume a fixed temperature of 300 K on the electrode and dielectric surfaces.
The boundary condition between the gas and the solid surfaces are given by[13,14] :

$$T_g = T_w + \lambda \left(\frac{\partial T}{\partial x} \right)_{wall} \qquad [23]$$

with

$$\lambda = \frac{2-\alpha}{\alpha} \xi \xi_0 \frac{T_{g(K)}}{p_{(Pa)} \sigma_{T(m^2)}} \qquad [24]$$

where α is the accommodation coefficient (equal to 0.5 in the calculations), ξ_0=0.6505 10^{-23}, σ_T is the cross-section for collisions between atoms (taken to be 20 10^{-20} m^2 in the calculations reported here), p is the gas pressure, T_g the gas temperature and T_w the wall temperature. ξ is given by:

$$\xi = \frac{c_p + \frac{5}{4}R}{c_p - \frac{1}{2}R} \qquad [25]$$

where c_p is the specific heat per mol at constant pressure and R the universal gas constant in units of J kg mol^{-1} K^{-1} (c_p=5/2 R for an atomic gas and therefore: ξ=1.875).
The accurate description of the ion heating in the sheath is difficult in the frame of a fluid model for ions, and the approximation of equation [22] together with the use of the boundary condition [23] seems un-consistent and is not very satisfactory. We performed a parametric study to estimate the consequences of these approximations (see section II). These assumptions need improvement in future work.

ANNEX II : To appear in Appl Phys Lett

Predicted properties of microhollow cathode discharges in xenon

J.P. Boeuf and L.C. Pitchford
Centre de Physique des Plasmas et Applications de Toulouse (CPAT), CNRS UMR 5002, 31061 Toulouse, France

K.H. Schoenbach
Center for Bioelectrics, Old Dominion University, Norfolk, VA, 23529, USA

Received August 26, 2004, accepted, xxx.

Abstract : A fluid model has been developed and used to help clarify the physical mechanisms occurring in MicroHollow Cathode Discharges (MHCD). Calculated current-voltage (I-V) characteristics and gas temperatures in xenon at 100 torr are presented here. Consistent with previous experimental results in similar conditions, we find a voltage maximum in the I-V characteristic. We show here that this structure reflects a transition between a low-current, abnormal discharge localized inside the cylindrical hollow cathode to a higher-current, normal glow discharge on the flat, front-face surface of the cathode. This transition, due to the geometry of the device, is a factor contributing to the well-known stability of MHCDs.

PACS: 52.50.Dg, 52.80.-s, 52.82.Hc

Considerable effort has been devoted over the past 10 years to the development of stable, high-pressure, non-thermal plasma sources. One discharge concept which has proven to be stable at atmospheric pressure and up to a power density of some 100 kW/cm^3 is the MicroHollow Cathode Discharge[1] (MHCD) developed by Schoenbach and coworkers. These discharges are created by applying a voltage between two electrodes in a geometry consisting of a cathode/dielectric/anode sandwich through which a hole is drilled. The thickness of the dielectric separating the electrodes and the diameter of the hole are both on the order of 200 microns. When arranged in an array, a large number of MHCDs can generate a high-pressure, DC, "surface plasma" with electron densities[2] up to 10^{13} cm^{-3}. A high-pressure DC[3], or pulsed[4], "volume plasma" can be generated with a third, planar electrode, located about a cm from the MHCD array. In this configuration the MHCD is used as an electron source for a larger volume discharge. Other high pressure plasma sources based on this idea are described in the review paper by Kunhardt[5] .

We present here first results from a simple model of a single MHCD. The aim of our work is to provide estimates of the main discharge and plasma parameters and to help understand the basic mechanisms governing the MHCD devices. The model used is based on solutions of fluid equations in the drift-diffusion approximation for the electron and ion transport coupled

with Poisson's equation. Dielectric boundary conditions are imposed on the open part of the computational domain to fix the boundary condition on the potential. This boundary is taken to be far enough from the active discharge region that it has no influence on the results. The ionziation rate coefficient appearing in the electron and ion source terms is supposed to depend on the mean electron energy[6] and an equation for the electron energy is added to the system of equations to be solved.

Gas heating leads to a decrease in the local neutral density and this can have important consequences on electron energy deposition in the sheath region and therefore on the sheath structure itself. Gas heating in a MHCD in xenon is mainly due to power deposition by ions in the sheath region (elastic and charge exchange collisions), but it is difficult to quantify the gas heating source term because a large part of the ion energy can be released on the cathode (by ions or fast neutrals) instead of in the gas[7]. In this first approach we consider that a given, fixed fraction of the ion heating is converted locally into gas heating, the rest being deposited on the cathode which is fixed at 300K. Using this as a source term, the gas temperature is obtained from the heat equation. Electron heating of the gas is taken into account but is negligable for our conditions, and gas flow is not taken into account.

To estimate the contribution of the xenon excited species to the overall ionization balance and the contribution of molecular ion formation and recombination to the overall electron loss, a very simple model kinetic is used. The species considered in the simulation are electrons, atomic ions, molecular ions, and metastable atoms. The model of the xenon metastable density is based on ref. 8, but simplified by assuming that the ratio of resonance to metastable atoms is constant.

The geometry of the MHCD used in the model calculations and its dimensions are given in Fig. 1 This geometry is similar to that used in the experimental work of Schoenbach et al[1]. The calculated current-voltage characteristic for a xenon discharge in this geometry at 100 torr is shown by the solid points in fig. 2. The following values were used for the parameters : secondary electron emission coefficient due ion bombardment, 0.002 and due to metastable bombardment, 0.005; fraction of ion power deposited locally in gas heating, 25%, surface temperatures , 300K; and ratio of resonance to metastable density, 0.1. While these values are estimates only, our quantitative predictions are not very dependent on these values, at least at 100 torr.

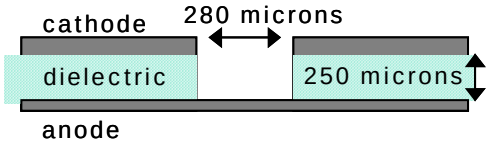

Fig. 1. Discharge geometry. The hollow cathode hole diameter is 280 microns, the electrodes are spaced by 250 microns, and each is 100 microns thick.

The shape of the calculated characteristic is similar to those measured by Schoenbach et al[1] in argon and by Moselhy and Schoenbach[9] in xenon. There is a steep increase in voltage at low current which is followed for increasing current by a region of negative slope and then a plateau. The region of negative slope was attribued by Schoenbach et al[1] to the onset of the classical hollow cathode effect. This interpretation was based in part on the calculations of Fiala et al[10] in argon hollow cathode discharges but for lower values of pd and where a marked decrease in the voltage was observed to be associated with efficient ionization due to electrons oscillating between opposite sheaths inside the hollow cathode; i.e., ionization due to pendulum electrons or the classical hollow cathode effect.

For the conditions of the calculations here, the structure in the I-V characteristic is not due to pendulum electrons because the electron energy loss mean free path is too short to allow electrons emitted from one part of the cathode to reach the opposite sheath with enough energy to ionize. Taking into account a decrease in gas density (ie an increase in mean free path) with increasing gas temperature, we estimate that gas temperatures greater than 1000K at 100 torr would be needed for penduluum electrons contribute to ionization. More detailed arguments will be presented e
lsewhere.

The voltage maximum observed in our calculations is associated with a transition from a glow discharge localized inside the hollow cathode (< 0.12 mA) to a glow discharge spreading along the outer cathode surface (> 0.12 mA). Thus, the steep slope of the I-V characteristic at low current corresponds to an abnormal glow discharge inside the hollow cathode; increasing current is achieved by increasing the current density. Above 0.12 mA, enough ions and metastables from the hollow cathode discharge reach the outer surface of the cathode to initiate a discharge between the outer cathode surface and the anode. Once initiated, this discharge is sustained ions and metastables created mainly in the volume outside the hollow cathode. This second discharge is in parallel with the first discharge localized inside the hollow cathode, and the I-V characteristic above 0.12 mA reflects the behavior of the normal glow discharge along the outer cathode surface. It is interesting to compare the MHCD characteristic with calculated characteristics of independent discharges inside the hollow cathode, curve (i) in fig. 2, and between the outer surface of the cathode and the anode in curve (ii), by setting γ to zero on different parts of the cathode surface.

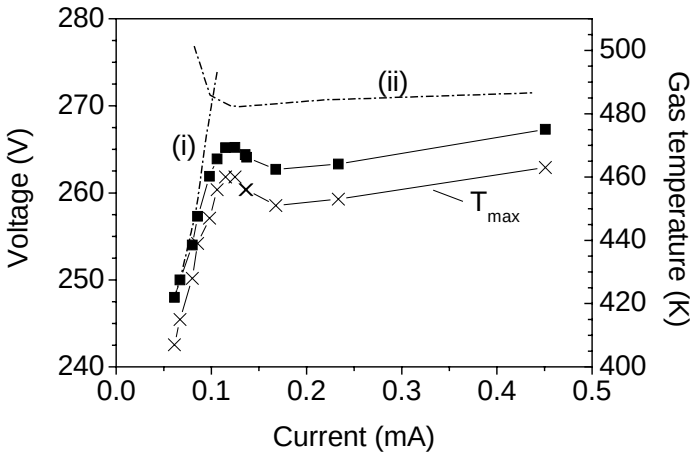

Fig. 2. Calculated I-V characteristic (solid symbols) and peak gas temperature (x) vs current. The dashed lines (i) and (ii) are characteristics calculated for discharge in the hollow cathode or between the cathode front fact and anode, respectively.

In fig. 3 we have plotted the line-of-sight emission intensity, calculated assuming each excitation event leads locally to the emission of one photon, for 3 different points along the I-V characteristic. Quantitatively, these results compare well with the experiments of Schoenbach et al[1]. At low current all excitation is well-localized inside the hollow cathode, and, abruptly above 0.12 mA, excitation is observed at radial positions greater than the hollow cathode radius. The on-axis peaks are the result of integrating through the positive column, and these are realtively more important with increasing current. The sharp, off-axis peaks in

the emission intensity inside the hollow cathode occur near the edges of the sheaths. See also ref. 11 for relevant experimental results at lower pressures.

Returning now to the plot of peak gas temperature T_{max} vs current in fig. 2, we see that T_{max} increases rapidly in the abnormal discharge regime below 0.12 mA where the ion current density at the inner walls of the hollow cathode is increasing. After the discharge has spread to the outer cathode surface, T_{max} tends to saturate, like the discharge voltage. The maximum gas temperature is always inside the hollow cathode. This saturation in the gas temperature is probably an important factor contributing to the stability of MHCDs.

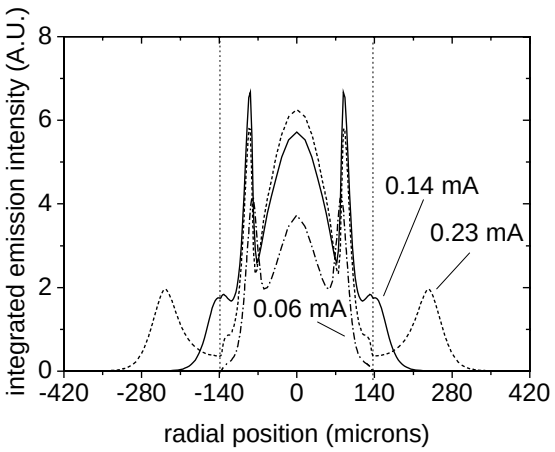

Fig. 3. Emission intensity integrated along the line of sight vs radial distance from the axis for three points along the baseline characteristic as indicated. The vertical lines show the position of the hollow cathode walls.

The peak plasma density at 0.12 mA is about $3x10^{13}$ cm^{-3}. On axis and inside the hollow cathode, 30% of the ions are molecular ions. The maximum metastable density is about $3x10^{14}$ cm^{-3} and its peak is off-axis near the sheath edges. Two-step ionization of the xenon metastables represents only about 10 to 15% of the total ionization.

Other calculations, not illustrated here, were made to estimate the effects of uncertainites in the gas heating source term and to better understand the effects of metastables. In all cases, we find the same general behavior of the MHCD but the detailed shape of the I-V curve depends on the exact values of the parameters used in the calculations. For example, the voltage maximum in the I-V characteristic is somewhat less pronounced and is shifted towards lower currents when a higher fraction of the ion power goes into gas heating. The peak gas temperature, T_{max}, is always inside the hollow cathode and for a given current, it is almost proportional to the voltage. T_{max} increases from 460K to almost 700K at 0.12 mA as the fractional ion power going into gas heating is increased from 25 to 100%. Note that the gas temperature (peak?) estimated in MHCDs in argon at 100 torr by Penache et al at[12] 0.5 mA (200 V) was about 500K, and we would expect the same discharge in xenon to be somewhat hotter because of lower thermal conductivity of xenon.

When metastable induced secondary electron emission from the cathode is set to zero, the I-V characteristic is shifted up to higher voltages, but the shape remains essentially the same. There is no voltage maximum present in calculations without metastables, but there is a sudden decrease in the slope of the I-V characteristic when the discharge spreads to the outer surface of the cathode.

Results of calculations for other gas pressures are similar to those presented above. One difference with experiment is that our model predicts an increase in voltage with gas pressure, whereas the opposite is found in experiments[9]. A process not accounted for in our model which could be important in this comparison is photoemission.

To summarize, although the model used here is approximate and more work needs to be done to improve the quantitative predictions, it is nevertheless useful for understanding the behavior of MHCDs. Our results show that with increasing current in MHCDs there is a transition from abnormal discharge inside the hollow cathode to a normal glow discharge where much of the current is drawn through the outer surface of the cathode. After the transition, the power deposited in the hollow cathode region does not increase significantly when the current increases, provided that the discharge can continue to spread on the outer surface of the cathode. This has implications for the discharge stability because the gas temperature (and electric field at the cathode surface – not shown here) tend to saturate with increasing current as long as there is available cathode surface for the discharge to spread.

Acknowledgements: This work was partially suppored by US Air Force through EOARD in London.

References:

1) KH Schoenbach, A El-Habachi, W Shi, and M Ciocca, Plasma Sources Sci. Technol. **6**, 468 (1997).
2) KH Schoenbach, A El-Habachi, MM Moselhy, W Shi, and RH Stark, Phys. Plasmas **7**, 286 (2000).
3) RH Stark and KH Schoenbach, J. Appl. Phys. **85**, 2075 (1999)
4) RH Stark and KH Schoenbach, J. Appl. Phys. **89**, 3568 (2001)
5) EE Kunhardt, IEEE Trans Plasma Sci. **28**, 189 (2000)
6) J-P Boeuf et LC Pitchford, Phys Rev E **51,** 1376 (1995).
7) I Revel, LC Pitchford, J-P Boeuf, J. Appl. Phys. **88**, 2234 (2000).
8) LC Pitchford, J Kang, C Punset, and J-P Boeuf, J. Appl. Phys. **92**, 6990 (2002)
9) MM Moselhy and KH Schoenbach, private communication, 2004.
10)A Fiala, LC Pitchford and J-P Boeuf, Proceedings of the XXII International Conference on Phenomena in Ionized Gases, Hoboken, NJ 1995, Contr. Papers 4, p. 191.
11) Th. Callegari, F Gegot, LC Pitchford, J Galy, J-P Boeuf, submitted to IEEE Trans Plasma Sci. 2004.
12) C Penache, M Miclea, A Brauning-Demian, O Hohn, S Schossler, T. Jahnke, K Keimax and H Schmidt-bocking, Plasma Sources Sci Tech, **11**, 476 (2002).

ANNEX III : To appear in IEEE Trans Plasma Sci

Special issue on Images in Plasma Science

Experimental Investigations of Glow Discharges in Hollow Cathode Geometries at Low Pressure

Th. Callegari, F. Gegot, L.C. Pitchford, J. Galy, J.P. Boeuf
CPAT, Univ P. Sabatier, 118 route de Narbonne, 31062 Toulouse, France

Abstract **- We present results of optical and electrical measurements of glow discharges in hollow cathode geometries in low pressure xenon. These are helpful for understanding results in microhollow cathode discharges operating at higher pressure.**

We present results of optical and electrical measurements of glow discharges in low pressure xenon in a hollow cathode geometry. This work is part of a larger project, the objective of which is to develop a better understanding of the operation and scaling of micro hollow cathode discharges, which have been shown to produce stable non-thermal plasmas at gas pressures up to atmospheric. The dimensions of the geometry chosen for the work here are proportional to those in the micro hollow cathodes of Schoenbach and colleagues [1], and the parameter pd (product of gas pressure and dimension) is in the same range (4 torr cm). Although the classical discharge scaling laws (same voltage V, pd,… for similar discharges) are valid only if non linear processes such as recombination, stepwise ionisation, temperature effects etc…, are negligible, we have found previously in our work on plasma display panels that simple experiments in "macro" configurations are very useful for understanding general properties of the discharge (discharge regime, current-voltage characteristics) in “micro” geometries [2].

The discharge geometry is shown in fig. 1. The hole diameter is 1 cm and the pressure is 4 torr, so pd is equivalent to a micro hollow cathode discharge at 200 torr with a 200 micron hole diameter.

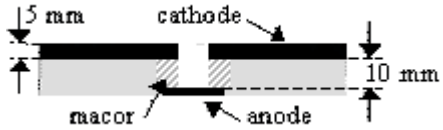

Fig. 1. “Macro hollow cathode” used for this work. Electrodes are in copper.

As previously seen in micro hollow cathode discharges [1] the V-I characteristic in our hollow cathode configuration (fig. 2) exhibits two different regions separated by a voltage peak. The voltage increases with current on the left of the peak and decreases on the right, with a tendency to form a plateau at higher current. The origin of this structure can be

interpreted with the six images displayed in Fig.3 (A to F) corresponding to 6 points along the V-I characteristic, as indicated. These images are photographs of the cathode face taken with a Princeton ICCD camera IMAX. The light is integrated over all wavelengths without corrections so these pictures show only qualitative features. The dotted white circles superimposed on the photographs in panels A,B and C represent the limit of the cathode hole. The photographs shown in panels D,E and F correspond to points on the right side of the voltage peak, and the second larger dotted white circle in these three panels shows the full cathode surface. Note the difference in scale between the first three and the second three panels.

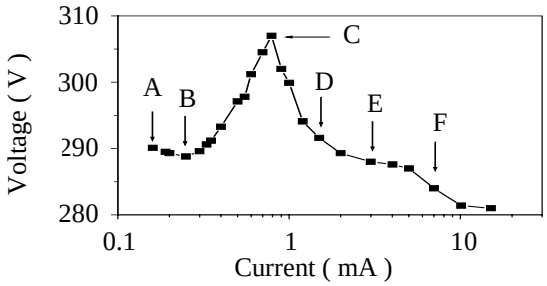

Fig. 2. Current voltage characteristic at 4 torr.

In spite of being qualitative, these photographs help understand the structure of the V-I curve. For currents below 0.8 mA, the discharge is well localized inside the cathode hole, and the shape of the V-I characteristic is typical of a normal (around 0.2 mA) and abnormal (between 0.2 and 0.8 mA) branch of a standard glow discharge. Above 0.8 mA, the discharge starts to spread along the cathode surface outside the hole, and the V-I characteristic is dominated by the discharge occurring between the back (flat) surface of the cathode and the anode. The ring of maximum intensity associated with the negative glow is very thin and close to the surface of the cathode inside the hole at 4 torr. The second, on-axis maximum in panel F is due to emission from the positive column.

Our recent model results [3] are consistent with these measurements, although the detailed structure of the calculated V-I characteristic is very dependent on the assumed secondary electron emission mechanisms and coefficients. Pd scaling of these results to smaller geometries is complicated by effects of gas heating and stepwise ionization of metastables. Nevertheless, these results are similar to those reported in micro hollow cathodes [1], and we suggest that the structure in the V-I curve in both geometries is related to the transition between a discharge inside and outside the cathode hole rather than to the onset of the hollow cathode effect.

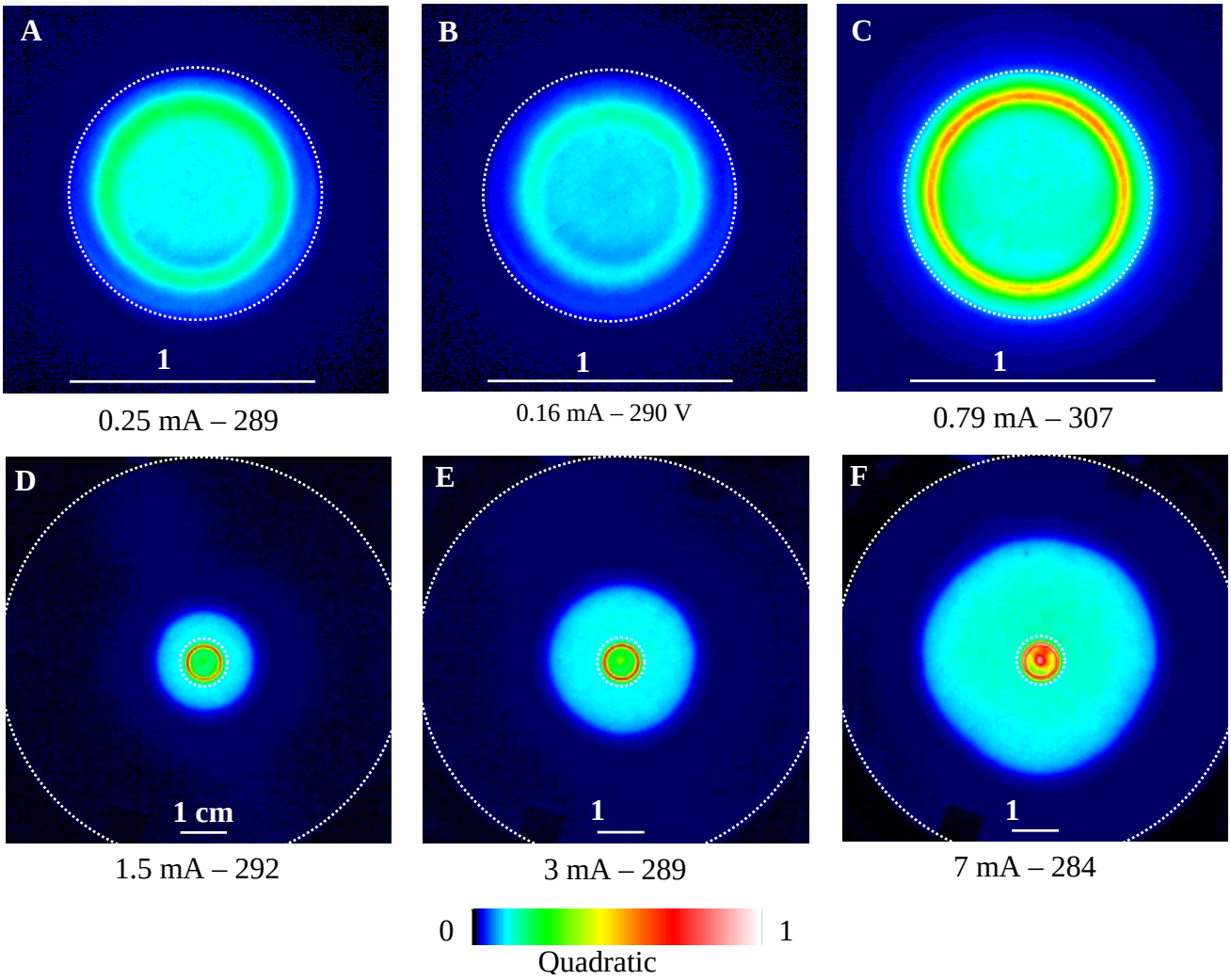

Fig. 3. Distribution of light intensity (300 nm – 900 nm) for 6 points in the 4 torr V-I curve (panels A to F). The dotted circles indicate the limit of the cathode hole in cases A, B, C and also the cathode surface in cases D, E and F. Note the difference in scale between the first three and the second three panels.

The authors gratefully acknowledge helpful discussions with Prof. K. Schoenbach. This work was partially supported by EOARD.

REFERENCES

[1] K. H. Schoenbach, A. El-Habachi, W. Shi, and M. Ciocca, Plasma Sources Sci. Technol. **6**, 468 (1997).
[2] T. Callegari, R. Ganter and J.P. Boeuf, J. Appl. Phys. **88**, 3905 (2000).
[3] J.P. Boeuf, L.C. Pitchford and K.H. Schoenbach, submitted to Appl. Phys. Lett. (2004).

ANNEX IV : Proceedings – Gas Disch Conf, 2005

Toulouse, September 2004

EXPERIMENTAL AND NUMERICAL INVESTIGATIONS OF GLOW DISCHARGES IN HOLLOW CATHODE GEOMETRIES: LOW PRESSURE AND HIGH PRESSURE SOURCES

Th. Callegari, F. Gégot, L.C. Pitchford, J. Galy, J.P. Boeuf

CPAT, Université Paul Sabatier, 118 route de Narbonne
31062 Toulouse cedex 4, France
callegari@cpat.ups-tlse.fr

ABSTRACT

An important research effort has been recently devoted to the development of non-equilibrium plasma sources at high pressures. Among the possible sources, the micro-hollow cathode discharges (MHCDs) have been shown to be able to sustain a non-equilibrium plasma up to atmospheric pressure and with good stability properties. The purpose of this paper is to study glow discharges in hollow cathode geometries and to better understand the operating regimes of these discharges. In this first approach we only consider low pressure and large dimensions hollow cathode discharges but with geometries similar to those used to generate atmospheric plasmas and with a scaling factor (typically 50) such that the pd product (pressure times dimensions) is the same as in the MHCD operating at high pressures.
We show that many properties of the low pressure hollow cathode discharges are very similar to those observed on the high pressure MHCDs, and that these discharges do not really operate in a so called "hollow cathode regime" (for pressure above 100 torr and hole diameter in the 100 μm range).

INTRODUCTION

Applications or potential applications of high pressure non equilibrium plasmas are numerous: plasma processing, UV sources, chemical or bacterial decontaminations of gases, micro chemical reactors, mirror and absorbers of microwave radiations etc… Considerable work has been done in the last 10 years to design stable, high-pressure, non-thermal plasma sources. A very promising concept for surface or volume high-pressure plasma sources is the Micro Hollow Cathode Discharge[1] (MHCD) developed by Schoenbach and coworkers at Old Dominion University. These discharges are formed through a ~ 200 μm diameter hole between two electrodes separated by a 200 μm dielectric layer. When arranged in an array, a large number of MHCDs can generate a high pressure, DC, "surface plasma" with electron densities[2] up to 10^{13} cm^{-3}. A high-pressure, DC[3], or pulsed[4], "volume plasma" can be generated with a third, planar electrode, located 1 or 2 cm from the MHCD array. In this configuration the MHCD is used as an electron source for a large volume discharge (other

high pressure plasma sources based on this idea are described in the review paper by Kunhardt[5]).

The purpose of this work is to better understand the physical properties of the discharge in hollow cathode geometries similar to those of Schoenbach et al.. In this first approach and for easier experimental investigations, a "macro-hollow cathode discharge" is studied. The dimensions of this device are about 50 times larger than those of the MCHDs of Schoenbach et al. and the operating pressure are 50 times lower. The geometry used in this paper is shown in Fig. 1. The hole diameter is 1 cm (instead of about 200 μm in the experiments of the Schoenbach's group) and the pressures in the 0.5-6 torr range (this corresponds to 25-300 torr for a micro-hollow cathode geometry). The gas considered in the experiments and in the calculations is pure xenon.

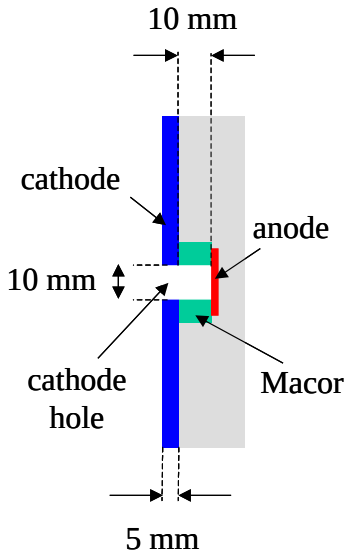

Figure 1 : "Macro" hollow cathode discharge geometry considered in this paper. The discharge forms between the inner wall of the cathode (hollow cathode) and the anode. At high enough currents the discharge spreads on the cathode surface outside the hole. The dimensions of the discharge (cathode-anode separation, hole diameter, thickness of the cathode are about 50 times larger than the dimensions of the micro-hollow cathode studied by the Schoenbach group. The electrodes are in copper.

Although it is clear that the classical discharge scaling laws (same voltage V, pd, E/p, j/p^2, … for similar discharges) are often not valid because of non linear processes such as recombination, stepwise ionisation, temperature effects etc…, we show in this paper that the general properties of the discharge (discharge regime, current-voltage characteristics) in the "micro" and "macro" configurations are very similar. Moreover we show that the simplicity of the experiments in the "macro" configurations helps understand, together with the numerical results, some of the features of the micro-hollow cathode discharges which were rather unclear up to now.

CURRENT VOLTAGE CHARACTERISTICS AND DISCHARGE PROPERTIES

Figure 2 shows the measured voltage-current characteristics of the discharge in the geometry of Fig. 1 and for different pressures.
For pressure above 2 torr, the measured current-voltage characteristics are very similar to those obtained in the micro-discharge configurations (see, e.g. Shi et al.[9])

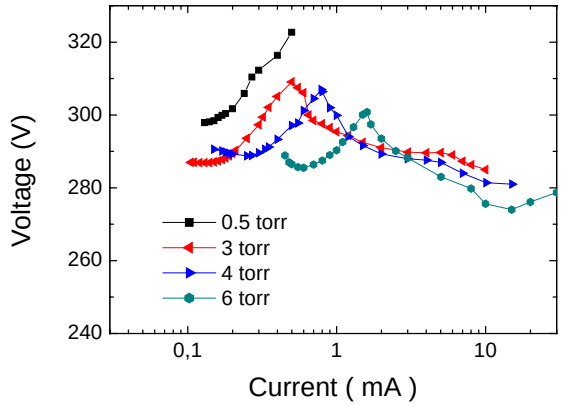

Figure 2 : Current-voltage characteristics of the "macro-hollow cathode discharge" for different pressures

As in the case of high pressure micro hollow cathode discharges, the current-voltage characteristics of the macro-hollow cathode discharge exhibit two different regions separated by a maximum. The maximum voltage shifts toward higher currents when the pressure increases. The voltage increases with current on the left of the maximum and the slope is negative on the right of the maximum, with a tendency to form a plateau at higher current. The voltage increases again when the current increases above a certain value (see the 6 torr curve).
This specific shape of the current-voltage curve and the transition from a positive to a negative slope has been interpreted by the Schoenbach group as a consequence of a hollow cathode effect (see, e.g. Ref. [6]). This interpretation was based on the fact that results of simulations in hollow cathode geometries published by Fiala et al.[7] predicted similar shapes of the I-V curve. The results of Fiala et al.[7] , based on the hybrid model of Ref. [8] were however obtained for lower pd products and we show in the modelling section below that the maximum in the I-V curves of Fig. 2 is actually not related to a hollow cathode effect. With rough estimations of the electron mean free path compared to the dimension of the hollow cathode, for example in the 6 torr discharge of Fig. 2, it is also easy to show that oscillations of fast electrons between the sheath in the hollow cathode ("pendulum effect") are not likely to occur.
Figures 3 and 5 show pictures of the discharge taken from top of the cathode with a Princeton ICCD camera IMAX. The light is just integrated on all wavelengths without corrections so these pictures only show some qualitative features. They are however very useful to help understand the shape of the I-V curve.
Figure 3 displays the I-V curve at 4 torr, with pictures of the light emitted by the discharge at 4 different points along the I-V characteristics. Figure 4 shows the radial intensity profiles in the same 4 cases.

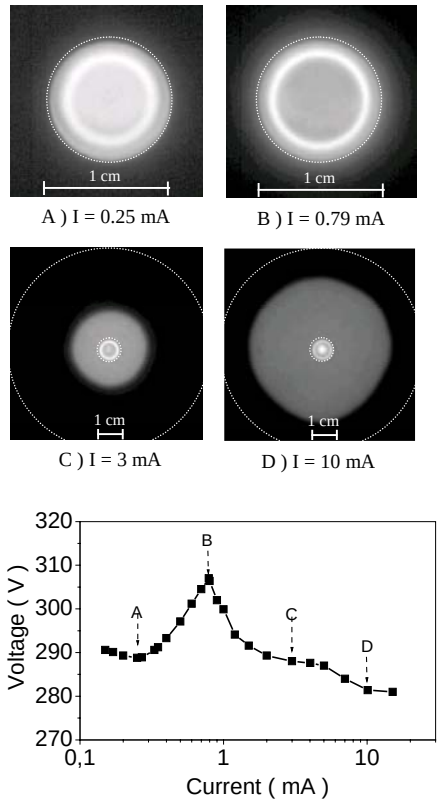

Figure 3 : Distribution of light intensity at 4 torr. View from top of the cathode for 4 different points on the I-V curve. The dotted circles indicate the border of the hole in A), B), C), D), and also the cathode limits in C) and D). Light emission appears only inside the hole in A) and B).

We see on Figs. 3 and 4 that for currents below the value (~0.8 mA, point B on the I-V curve) at the peak voltage, the discharge is inside the cathode hole (see Fig. 1). Only the part of the cathode inside the hole contributes to the discharge current. The shape of the I-V characteristics below 0.8 mA is typical of a normal (around 0.2 mA) and abnormal (between 0.2 and 0.8 mA) branch of a standard glow discharge. Above 0.8 mA, the discharge starts to spreads on the cathode outside the hole and the I-V characteristics becomes dominated by the discharge between the back (flat) surface of the cathode and the anode. The fact that the slope of the I-V curve above 0.8 mA is negative is related to the discharge geometry and to the presence of metastable atoms (this will be discussed in details in a forthcoming paper).

The distribution of light emission inside the hole in the 4 torr case (Figs. 3 and 4) exhibits a ring and a maximum in the center. The ring is associated with the negative glow corresponding to the part of the cathode inside the hole. The maximum of light emission in the center of the hole is related to the positive column between the negative glow and the anode. The relative intensity of the positive column light increases with increasing current. As can be seen in Figs. 3 and 4, the ring of light is very close to the surface of the cathode inside the hole and is very thin. This gives an indication of the relatively small sheath length and negative glow length and confirms that there cannot be any “pendulum electrons” oscillating between the sheaths inside the hole, under these conditions. Using the scaling mentioned above, the conditions of Fig. 3 correspond to a pressure of about 200 torr in the conditions of the micro-hollow cathode geometries of Schoenbach et al.

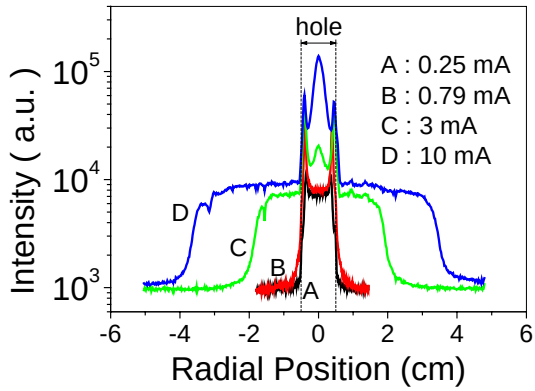

Figure 4 : Measured distribution of light intensity at 4 torr as a function of radial position for the 4 points on the I-V curve of Fig. 3.

The hollow cathode effect and the “pendulum electrons” appear at lower pressures, for example at 0.5 torr in the macro hollow cathode discharge studied in this work (~25 torr in the micro-hollow cathode geometries of Schoenbach et al.).

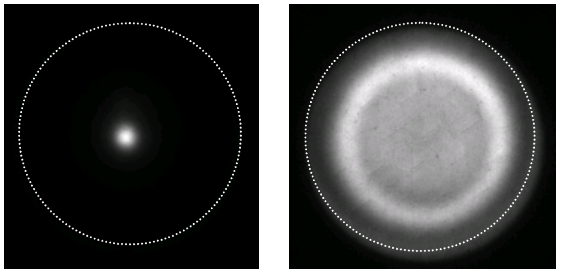

0.5 torr, 0.14 mA 4 torr , 0.16 mA

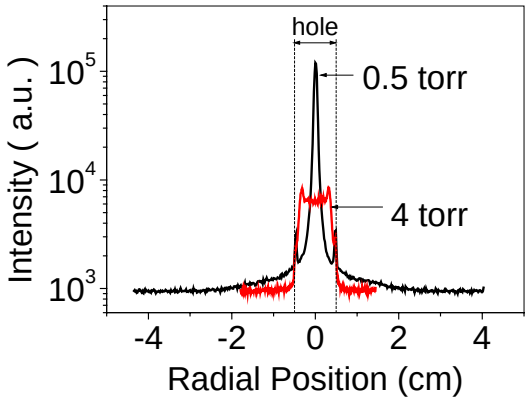

Figure 5: Comparison of the measured distribution of light intensity at 0.5 torr and 4 torr for similar values of the current.

Figure 5 shows the I-V characteristics together with some pictures of light emission in the macro hollow cathode discharge at 0.5 torr and 4 torr for values of the current such that the discharge is inside the hole. It is clear that in the 0.5 case, the negative glows corresponding to the sheaths inside the hole overlap and only one peak in the light intensity is visible. In the 4 torr case, the negative glows are clearly separated and do not overlap (the light in the center of the hole comes from the positive column between the cathode hole and the anode). From this comparison we can deduce that the hollow cathode effect is effective at 0.5 torr and not at 4 torr.

SIMULATION RESULTS

We have used both a hybrid fluid-Monte Carlo model (similar to the one used in Ref. [8]), and a fully fluid model with an energy equation for electrons as in [9] but with an improved numerical treatment of the energy equation as in [10], and a semi-implicit coupling of the Poisson and transport equations.

A simplified model of the excited species kinetics for xenon was used where the metastable and resonant states of xenon as well as the molecular xenon ions were included (in a similar way as in [11].

Secondary electron emission from the cathode due to ion (coefficient γ_i) and metastable atom (coefficient γ^*) impact was taken into account in the model.

Figure 6 shows two examples of calculated I-V curve for a pressure of 3 torr.

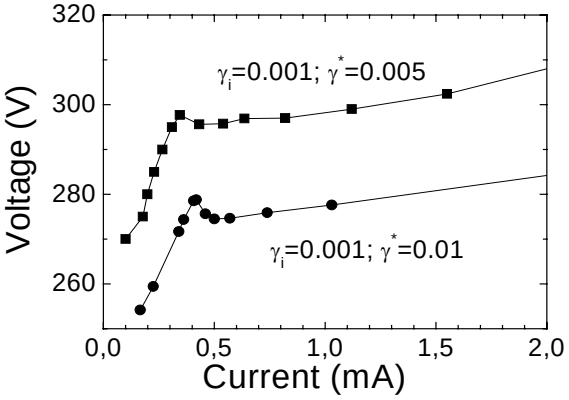

Figure 6: Simulated current-voltage characteristics at 3 torr (fully fluid model) for two values of the secondary emission coefficients

We see in Fig. 6 that the I-V curves present two regions with different slopes and exhibit a maximum which depends on the secondary emission coefficients. The current voltage characteristics curves are qualitatively very similar to the measured one (Fig. 2) although the region with negative slope is less pronounced in the model. The model results also show (see Fig. 7 and compare with Fig. 4) that the change in the slope and the maximum of the I-V curve correspond to the point where the discharge moves from inside the cathode hole to the external surface of the cathode.

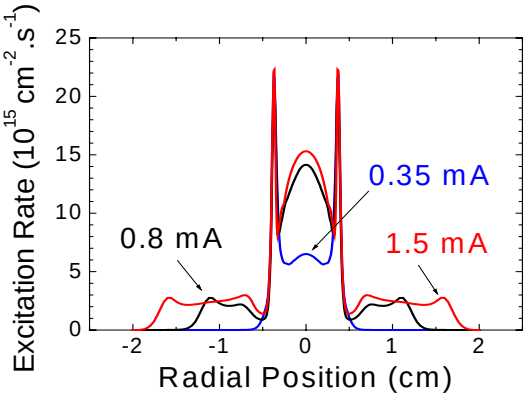

Figure 7: Calculated (fully fluid model) radial distribution of the total xenon excitation rate at 3 torr and for 3 values of the current along the characteristics of Fig. 6 (for γ_i=0.001 and γ^*=.005).

Calculations with the hybrid fluid-Monte Carlo model (Fig. 8) show that the hollow cathode effect is clearly present at 0.5 torr but disappear above 2 torr (the two negative glows are clearly separated).

CONCLUSION

The experimental and simulation results described in this paper clarify the discharge regimes in hollow cathode geometries similar to those studied by the Schoenbach group.

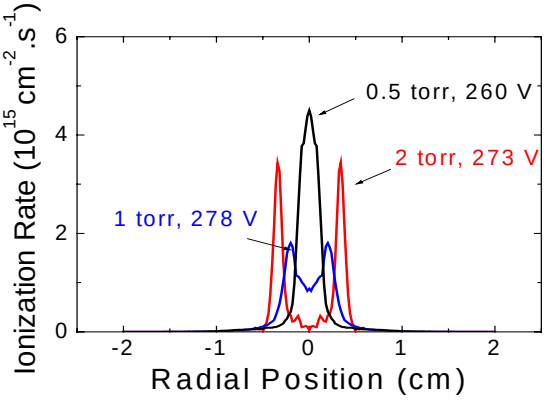

Figure 8: Radial distribution of the ionization rate obtained with the hybrid Monte Carlo – fluid model for three values of the pressure (γ_i=0.001, metastable not included).

The results show that in xenon, the hollow cathode effect due to "pendulum electrons" should occur only at pressures typically less than 100 torr in geometries with 200 μm hole diameter (2 torr in our "macro-hollow cathode" geometry, with 1 cm hole diameter). The presence of a maximum in the current-voltage characteristics is not due to the hollow cathode effect but to a transition between two regimes of the discharge, inside and outside the cathode hole, and with a possible role of metastable atoms.

ACKNOWLEDGMENTS

The authors would like to thank Prof. K. Schoenbach and M. Moselhy for helpful discussions and for sharing their experimental, unpublished data. This work (modeling part and interpretation) has been partially supported by US Air Force (Grant 03383).

REFERENCES

[1] KH Schoenbach, A. El-Habachi, W. Shi, and M. Ciocca,, Plasma Sources Sci. Technol. 6, 468 (1997)

[2] KH Schoenbach, A. El-Habachi, MM Moselhy, W Shi, and RH Stark, Phys. Plasmas 7, 286 (2000).

[3] RH Stark and KH Schoenbach, J. Appl. Phys. 85, 2075 (1999)

[4] RH Stark and KH Schoenbach, J. Appl. Phys. 89, 3568 (2001)

[5] EE Kunhardt, IEEE Trans Plasma Sci. 28, 189 (2000)

[6] W. Shi, R. Stark, and K. Schoenbach, IEEE Trans. Plasma Sci. 27, 16 (199)

[7] A. Fiala, L. C. Pitchford, and J. P. Boeuf, in *Proc. XXII Conf. Phenomena Ionized Gases*, Hoboken, NJ, 1995, vol. 4, pp. 191–192.

[8] J.P. Boeuf and L.C. Pitchford, IEEE Trans. Plasma Sci. 19, 226 (1991)

[9] J. P. Boeuf et L. C. Pitchford, Phys Rev E 51, 1376 (1995).

[10] G.J.M. Hagelaar and G.M.W. Kroesen, J. Comp. Phys. 159, 1 (2000)

[11] L.C. Pitchford, J. Kang, C. Punset, and J.P. Boeuf, J. Appl. Phys**.** 92**,** 6990 (2002)